eLife

Reviewed Preprint
v2 • December 24, 2024
Revised by authors

Reviewed Preprint
v1 • August 22, 2024

Neuroscience

Activity-dependent lateral inhibition enables the synchronization of olfactory bulb projection neurons

Tal Dalal, Rafi Haddad

The Gonda Multidisciplinary Brain Research Center, Bar-Ilan University, Ramat-Gan, Israel

eLife Assessment

This **important** study uses optogenetics in combination with single cell recordings to selectively activate sensory input channels within the olfactory bulb, providing direct evidence for activity-dependent and distance-independent enhancement of stimulus-evoked gamma oscillations via lateral interactions between input channels, most likely via granule cells. The article presents **solid** evidence to support the main conclusions.

https://doi.org/10.7554/eLife.100141.2.sa3

Abstract

Information in the brain is represented by the activity of neuronal ensembles. These ensembles are adaptive and dynamic, formed and truncated based on the animal's experience. One mechanism by which spatially distributed neurons form an ensemble is by synchronizing their spike times in response to a sensory event. In the olfactory bulb, odor stimulation evokes rhythmic gamma activity in spatially distributed mitral and tufted cells (MTCs). This rhythmic activity is thought to enhance the relay of odor information to the downstream olfactory targets. However, how specifically the odor-activated MTCs are synchronized is unknown. Here, we demonstrate that optogenetic activation of one set of MTCs can gamma-entrain the spiking activity of another set. This lateral synchronization was particularly effective when the recorded MTC fired at the gamma rhythm, facilitating the synchronization of only the substantially active MTCs. Furthermore, we show that lateral synchronization did not depend on the distance between the MTCs and is mediated by granule-cell layer neurons. In contrast, lateral inhibition between MTCs that reduced their firing rates was spatially restricted to adjacent MTCs and was not mediated by granule-cell layer neurons. This dissociation between these two interaction types suggests that they are mediated by different neural circuits. Our findings propose a simple yet robust mechanism by which spatially distributed neurons entrain each other spiking activity to form an ensemble.

Highlights

1. MTC activation entrains the spike timing of other MTCs in an activity-dependent and distance-independent manner.
2. MTC to MTC suppression is activity- and distance-dependent
3. Spatially distributed Granule cell layer neurons control MTC's spike timing, yet do not substantially affect their odor-evoked firing rate.

Introduction

Information in the brain is represented by the activity of ensembles of neurons, typically interconnected through a network of interneurons (Buzsáki and Chrobak, 1995). These interactions reshape the ensemble activity as it evolves in time and space. One mechanism by which spatially distributed neurons form an ensemble is by synchronizing their spiking activity in response to a sensory event (Buzsáki, 2010). This synchronization is thought to enhance the transmission of information to downstream targets (Dalal and Haddad, 2022; Macleod et al., 1998; Pritchett et al., 2015; Sohal, 2016).

Olfactory processing starts with the activity of odorant-activated olfactory sensory neurons. The axons of these sensory neurons terminate in one or two anatomical structures called glomeruli located on the surface of the olfactory bulb (OB). Each glomerulus is innervated by several MTCs, which then project the odor information to several cortical regions. Different odors activate different olfactory receptors. The odor-activated MTCs interact with each other via a dense network of inhibitory neurons spanning all OB layers (Burton, 2017). Several studies have shown that odorants evoke strong spike gamma-entrainment in MTCs (Beshel et al., 2007; Dalal and Haddad, 2022; Fukunaga et al., 2014; Lepousez and Lledo, 2013), as well as synchronous firing of MTCs (Doucette et al., 2011; Kashiwadani et al., 1999). This synchronization is likely to be mediated by granule cells (GCs) (Schoppa, 2006) located in the granule cells layer (GCL) and has recently been shown to enhance odor-information transmission to the Piriform cortex (Dalal and Haddad, 2022). However, the mechanism by which specifically the odor-activated MTCs are synchronized is unknown. One prominent hypothesis is that GCs enable synchronization solely between odor-activated MTCs via an activity-dependent mechanism for GABA-release (Egger and Kuner, 2021; Lage-Rupprecht et al., 2020).

GCs are the most abundant type of neuron in the OB. They form dendrodendritic synapses with MTCs (Shepherd, 2004) and, via these synapses, can provide recurrent and long-range lateral inhibition. Earlier studies that were not aware of the role of EPL interneurons in regulating MTC spiking activity, suggested that GCs mediate lateral inhibition between MTCs that can suppress their firing rates (Arevian et al., 2008; Giridhar et al., 2011; Yokoi et al., 1995). In contrast, more recent studies demonstrated that in-vivo lateral suppression of MTC firing rate is sparse and weak (Fantana et al., 2008; Lehmann et al., 2016; Pressler and Strowbridge, 2017). Consistent with this weak effect on MTC firing rates, one study showed that optogenetically silencing the GCs did not affect odor-evoked inhibitory responses (Fukunaga et al., 2014). These findings cast doubt on the role of GCs in suppressing MTCs' odor-evoked firing rate (Burton, 2017).

Here, we used odor and optogenetic stimulations of MTCs and GCL neurons in anesthetized mice, to study how active MTCs interact to regulate their spikes timing and firing rates. We found that MTCs form two dissociated types of interactions. One interaction enables the synchronization of only activated MTCs dispersed on the OB surface and is mediated by GCL neurons. The other type of interaction affecting MTCs firing rate is limited to relatively nearby MTCs, and, contrary to some common views in the field, is not mediated by GCL neurons.

Results

Activity-Dependent Lateral Synchronization of MTCs

To investigate how MTCs interact we expressed the light-gated channel rhodopsin (ChR2) exclusively in MTCs by crossing the Tbet-Cre and Ai32 mouse lines (Grobman et al., 2018; Haddad et al., 2013), and extracellularly recorded the spiking activity of MTCs in anesthetized mice during optogenetic stimulation using tungsten electrodes. We first mapped each recorded cell's receptive field, i.e., the set of MTCs on the dorsal OB that affect its firing rates when light-stimulated. Pseudo-random light patterns composed of multiple light spots were projected over the OB surface (**Supplementary Figure 1a**) and the spike-triggered-average was computed to obtain the receptive field map (**Figure 1a**; 'STA', see Methods). Light patterns comprised of 5-10 multiple light spots of size 88-110 μm^2. This stimulation protocol ensured the activation of varied MTC combinations associated with different glomeruli, among them the MTC we recorded from. As expected, light-stimulating the area above the recording electrode activated the recorded MTC (the 'hotspot'). This protocol also revealed regions on the OB surface that had a suppressive effect on the activity of the recorded MTC (**Figure 1a**). Based on the receptive field map, we selected several spots and light-stimulated them either alone or simultaneously with the 'hotspot' using four increasing light intensities (**Figure 1a-b**; N = 5 mice; 27 well-isolated single units; overall 127 pairs were tested, 2-8 different pairs per cell; see Methods for spots selection criteria). We found that in a subset of neurons, paired light activation precisely aligned the spike times of the recorded MTC across trials (**Figure 1c**), giving rise to a gamma rhythm (**Figure 1d-e**). To quantify the change in spikes gamma entrainment at the population level, we computed the difference in the area under the power spectrum density (PSD) curve between the two conditions at the gamma range (40-70Hz, **Supplementary Figure 1b**; see Methods). We found that the change in entrainment was significantly higher than zero (**Figure 1f**; $P < 0.001$ and $P = 0.13$ for real and shuffled data, respectively; two-tailed paired *t*-test, N = 319/511 values from all pairs and light intensities that significantly responded to light stimulation). Overall, we found that in ~16% of the stimulated pairs, paired light-activation significantly enhanced the gamma entrainment (N = 50/319 values that exceeded the 95% confidence interval of the shuffled distribution, colored in brown in **Figure 1f**). Varying the light intensities revealed that the enhanced gamma entrainment was most effective when the postsynaptic MTC firing rate was ~40Hz (**Figure 1g**). Analyzing the locations in which paired activation significantly increased the temporal precision revealed no significant correlation between the pair's distance and its gamma entrainment change, suggesting that lateral entrainment is driven by MTCs across the glomerular map without any discernable spatial organization (**Figure 1h**; $r = 0.05$, $P = 0.73$, Spearman correlation). Overall, we found activity-dependent enhancement of MTC spike precision in the gamma range that is distance-independent.

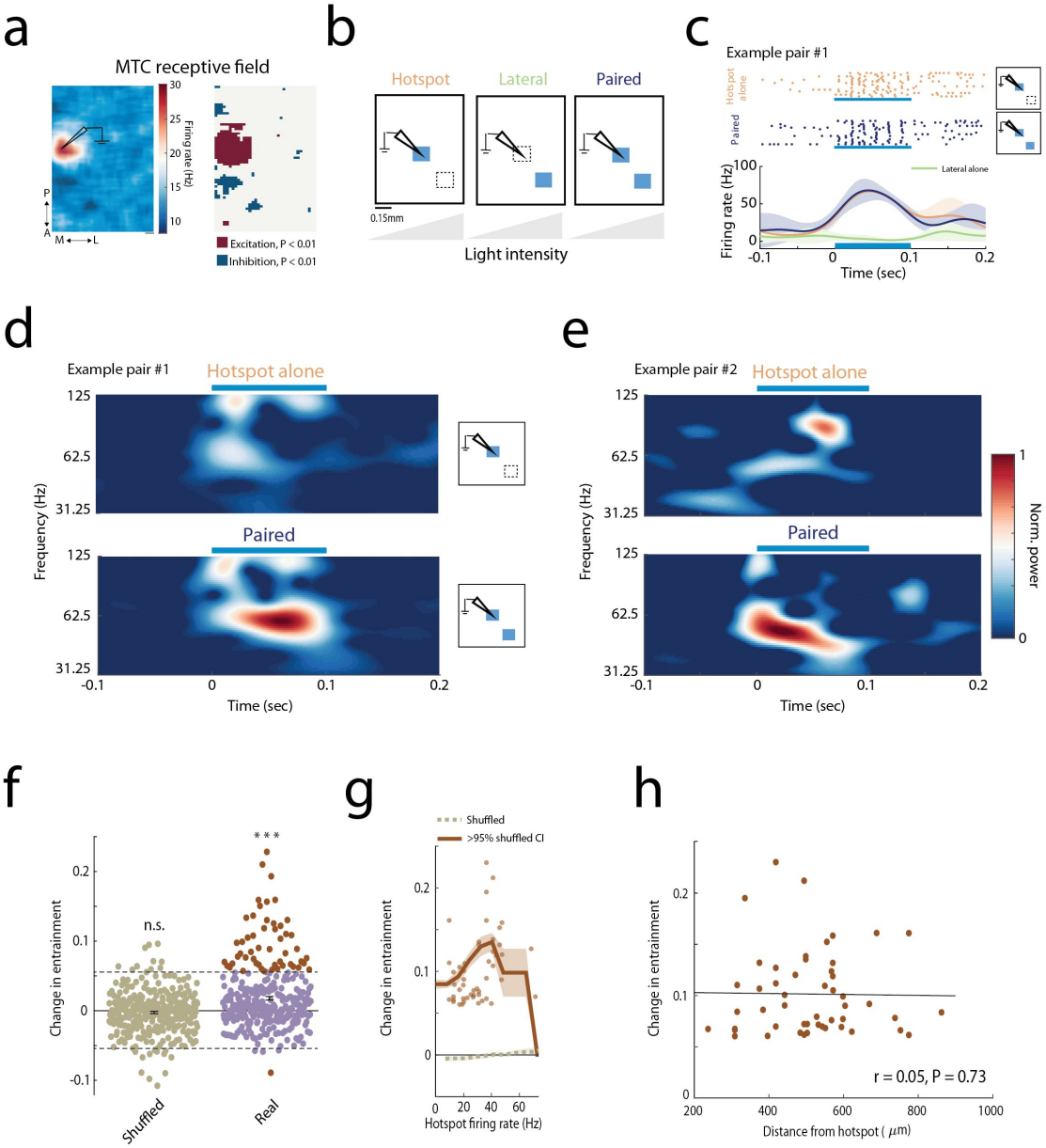
a
MTC receptive field
Firing rate (Hz)
Excitation, P < 0.01
Inhibition, P < 0.01
b
Hotspot
Lateral
Paired
0.15mm
Light intensity
c
Example pair #1
Lateral alone
Firing rate (Hz)
Time (sec)
d
Example pair #1
Hotspot alone
Paired
Frequency (Hz)
Time (sec)
e
Example pair #2
Hotspot alone
Paired
Frequency (Hz)
Norm. power
Time (sec)
f
Change in entrainment
n.s.
Shuffled
Real
g
Shuffled
>95% shuffled CI
Change in entrainment
Hotspot firing rate (Hz)
h
Change in entrainment
r = 0.05, P = 0.73
Distance from hotspot (μm)

Figure 1

Activity-dependent lateral-entrainment of spike times

a) Left: STA map with an excitatory region near the electrode location and presumably several surrounding inhibitory spots. Right: the significance map ($P < 0.01$ relative to shuffled data, see Methods). Scale bar, 0.1mm.

b) Schematic illustration of the experimental setups. Photo-stimulation of each spot alone (hotspot or lateral spot conditions marked by orange and green text, respectively) or paired stimulation (marked in blue) using four different light intensities.

c) Raster plots and smoothed PSTHs of the response to light stimulation of the hotspot (top, orange) and paired stimulation (middle, blue). Note, the increase in spike time accuracy within and across trials when both spots are activated (middle panel). Paired light stimulation did not affect the average firing rate in this example (lower panel). The effect of light stimulation of the lateral spot alone is shown in green.

d-e) Examples of MTCs time-frequency wavelet analysis from two different mice. Example pair #1 is the pair displayed in **c**. Both examples show a strong gamma rhythm following paired stimulation. In pair #1, gamma power peaked at ~58Hz, and pair #2 at ~48Hz.

f) Paired stimulation increases spikes' temporal precision. Mean ± SEM of the change in spikes entrainment at the population level (N = 319/511 values from all pairs and light intensities that significantly responded to light stimulation, $P = 0.13$ and $P < 0.001$ for shuffled (green) and real (purple) data, respectively; two-tailed paired *t*-test). In brown are values that exceeded the 95% confidence interval of the shuffled data distribution values of increased and decreased spike entrainment, respectively; confidence interval is marked by dashed black lines).

g) Lateral entrainment is activity-dependent. The moving average of the data shown in **f** is plotted as a function of the firing rate of the postsynaptic MTC (N = 50 values of increased entrainment). The increase in entrainment was largest when the neuron fired at ~40Hz. The color code is the same as in **f**. The shuffled data is shown in a dashed green line.

h) Spike entrainment does not depend on the distance between the MTC pair. No significant correlation was found between the increase in spike-entrainment and the distance from the hotspot ($r = 0.05$, $P = 0.73$, Spearman correlation; N = 50 values with significant increase in spike entrainment, brown dots in **g**).

Activity-Dependent Lateral Suppression of MTCs is Confined in Space

In addition to lateral synchronization between co-active MTCs, we found that paired activation could suppress the recorded MTC firing rate (termed here as lateral suppression, **Figure 2a-b**). **Figure 2c** shows the response of a recorded MTC when light-stimulated alone and simultaneously with other MTCs under four different light intensities (pair #1 or pair #2, as marked in **Figure 2a**). Activation of pair #1 evoked lateral suppression that was dependent on the recorded MTC firing rate, while activation of pair #2 did not affect the MTC firing rate for the four light intensities tested . Plotting the evoked change in firing rate caused by paired stimulation as a function of the MTC firing rate when stimulated alone revealed that lateral suppression is most effective when the recorded MTC fires in the gamma range (i.e., ~30-80 Hz, **Figure 2d**). Light stimulating the lateral spots alone did not affect the MTC baseline firing rate (**Supplementary Figure 2a**). Overall, in 19% (24/127) of the tested MTC pairs, the recorded MTC firing rate was significantly suppressed during paired stimulation compared to hotspot stimulation alone. In contrast to the lack of spatial organization between MTC pairs that caused spike entrainment, we found a significant correlation between the distance of the paired spots and

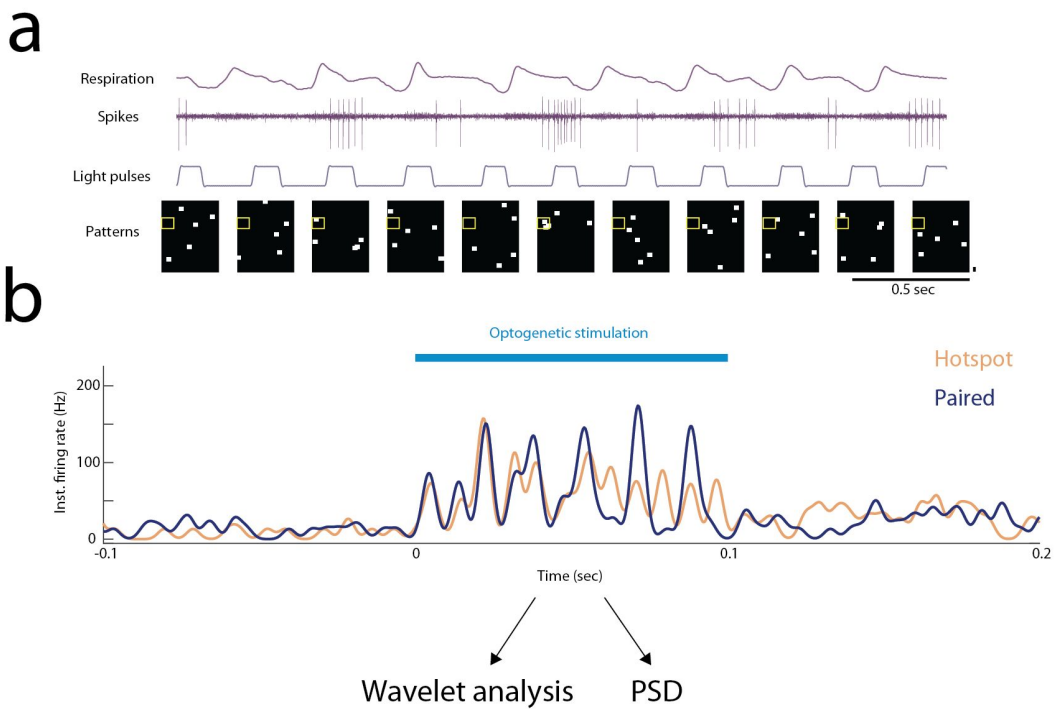

Supplementary Figure 1

Paired MTC activation induces spikes entrainment

a) Light stimulation protocol. An image containing N randomly distributed light patches (N = 5 in this example) is projected on the dorsal bulb in each trial. The light patterns are shown in the bottom panel. The yellow rectangle marks the region around the recording electrode. The spiking activity and the respiratory signal are shown above. Multiplying each pattern by the firing rate it evoked and averaging across all trials gives the STA activity map (see Methods). Scale bars: 0.5 second; 110 μm.

b) A description of the analysis used to compute the spikes entrainment. For each condition (hotspot alone or paired activation) a PSTH was computed using a Gaussian window of 2 ms. We then fed this PSTH into the wavelet analysis (as shown in **Figure 1d-e**, see Methods) and computed the power spectral density (PSD) using a Multitaper analysis during the stimulus presentation (100ms, see Methods).

the level of evoked suppression (**Figure 2e**; r = 0.45, P = 0.001, Spearman correlation), consistent with a recent study (Peace et al., 2024). To further verify that lateral inhibition is limited to proximal MTCs, we analyzed the inhibition found in the receptive field (STA) maps. Centering all z-scored maps relative to the 'hotspot' location (N = 27 neurons from 5 mice) revealed that MTC-to-MTC suppressive interactions are strongest and densest in regions that are adjacent to the recorded MTC (~400 μm) and diminished beyond that (**Figure 2f** and **Supplementary Figure 2b**). Furthermore, computing the STA maps while excluding the light patterns that contained a light spot that hit the electrode location ('hotspot' area) resulted in maps that did not contain suppressive regions (**Supplementary Figure 2c-d**). This analysis further confirms that lateral suppression requires the recorded MTC to be active. In summary, we show that MTC-to-MTC suppressive interactions are spatially confined and activity-dependent.

Two different neural circuits mediate spikes suppression and entrainment

In our experimental design, the same MTC participated in more than one pairing. Analyzing these pairs revealed that while light stimulation of one pair could enhance the spike precision without affecting its firing rate, activation of a different pair at the same light intensity could suppress the MTC firing rate without affecting its spike precision (**Figure 3a**). Furthermore, light-activating the same pair with two different intensities could suppress the MTC firing rate at one intensity and enhance spike entrainment in the second (**Figure 3b**). To quantify these effects at the population level, we compared the firing rate change between pairs that evoked significant inhibition and these that evoked spikes entrainment, and found a significant difference between the two groups (**Figure 3c**, P < 0.001, two-tailed *t*-test). Consistently, we found only a minor overlap between the groups, suggesting that pairs that exhibit spikes entrainment typically do not exhibit lateral suppression (**Figure 3d**). These findings suggest that spike suppression and entrainment are not features of the recorded cell type (i.e., mitral versus tufted cells) but instead reflect two different circuits that interconnect MTCs.

Optogenetic activation of GCL neurons increases MTC synchrony in an activity-dependent and location-independent manner

We next sought to understand the neural circuits that mediate spike entrainment and suppression. We examined whether GCL neurons-MTC interactions underlie the temporal changes or the suppressive interactions we found. We conditionally expressed ChR2 in GCL interneurons by injecting AAV5-EF1a-DIO-ChR2 to Gad2-Cre mice into the GC layer (**Figure 4a**) as in (Dalal and Haddad, 2022; Fukunaga et al., 2014). We used odor stimuli to activate the recorded MTC, while recording MTC spiking activity and the LFP (**Supplementary Figure 4a**). To optogenetically activate the GCL neurons belonging to a glomerulus column, we used a relatively large light spot sized ~330 μm^2 (Egger and Urban, 2006). We then tested how light-activation of subsets of GCL neurons at different locations affects MTC odor-evoked temporal dynamics and spike rate suppression (**Figure 4b**; N = 4 mice, N = 31 cell-odor pairs from 22 cells). To examine the temporal effects, for each cell-odor pair we extracted the MTC odor-evoked spike phases of the LFP-gamma cycles across all trials. We then quantified the level of spike-LFP gamma coupling using the pairwise phase consistency measure (PPC1). This measure minimizes the bias of the neuron's firing rate on the spike-LFP synchrony value (Vinck et al., 2012). Only MTCs that were excited by the odor were analyzed (N = 18/31, P < 0.05, two-tailed paired *t*-test). We found that light-activating GC-columns significantly increased MTC spike phase-locking (**Figure 4c**, N = 3 light spots for each cell-odor pair, a total of 54 light spots tested, P = 0.0016, two-tailed paired *t*-test. Furthermore, within the distance range that we were able to measure, the increased phase-locking did not significantly correlate with the distance from the MTC, and depended on the level of the MTC firing rate (**Figure 4d-e**). Plotting the odor-evoked spikes of an example high-firing neuron by aligning them to an arbitrary spike in each trial as done in (Fukunaga et al., 2014) further

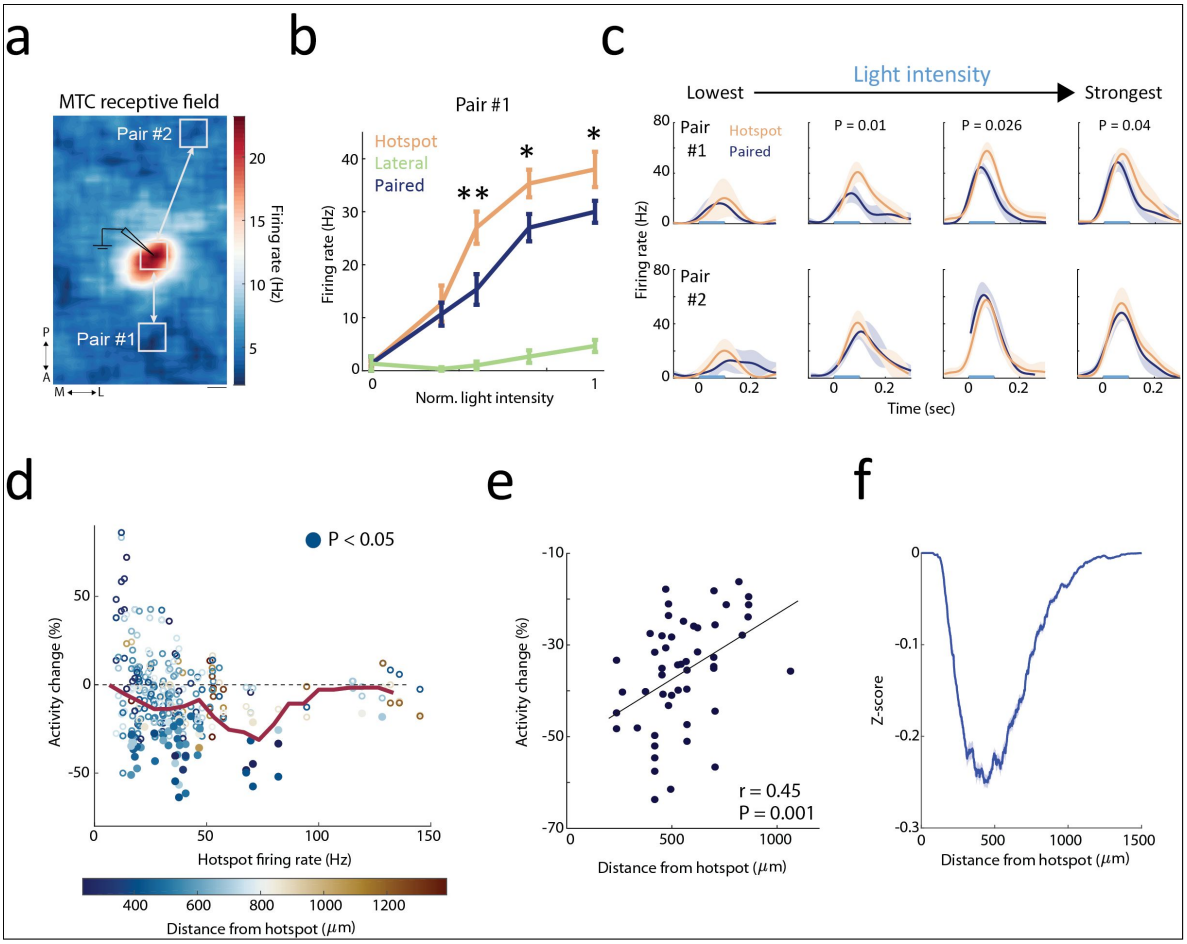

Figure 2

Activity-dependent lateral suppression of MTCs is confined in space

a) An example of a MTC receptive field (STA map). The white rectangles mark the spots exposed to light stimulations. The hotspot location is marked with an electrode drawing. Scale bar, 0.1mm.

b) Mean ± SEM firing rates of light stimulating pair #1 from **a** for each of the three conditions across all four light intensities. Activation of pair #1 (blue) caused a reduction in the recorded MTC firing rates only when the recorded MTC fired above ~25 spikes/sec. Zero denotes the baseline firing rate. *P < 0.05, **P < 0.01, two-tailed paired *t*-test.

c) PSTHs of pair #1 and #2 responses to light stimulations at four different light intensities. Paired stimulation of pair #1 evoked activity-dependent suppression. Paired stimulation of more distant neurons in pair #2 did not affect the recorded MTC firing rates for all tested light intensities. Light stimulation is marked with a blue bar (0.1 sec). PSTHs without a p-value showed no significant change between the firing rates of paired stimulation and hotspot stimulation alone.

d) Summary analysis of the effect of paired activation on MTCs firing rate. Each point marks the percentage change in firing rate (Y-axis) relative to the firing rate elicited by light stimulating the hotspot alone (X-axis). Suppressive effects (i.e., negative activity change) occurred mainly when the MTC fired in the gamma range (~30-80 Hz). Color code denotes the distance between the light-activated MTC pair. Filled circles mark significant activity change (P < 0.05, two-tailed unpaired *t*-test, N = 51/319 data points). The red line shows the moving average. Only light intensities that elicited a significant light response were analyzed (319/511; P < 0.05, two-tailed paired *t*-test).

e) Lateral suppression degrades with distance. Spearman correlation between the change in firing rate for all significant inhibitory pairs (the filled circles in **d,** N = 51) and their distance to the hotspot (r = 0.45, P = 0.001).

f) Z-score Mean ± SEM change in MTC activity across all STA maps superimposed and centered relative to the 'hotspot'. The centered map is shown in **Supplementary Figure 2b**. Zero denotes the hotspot location.

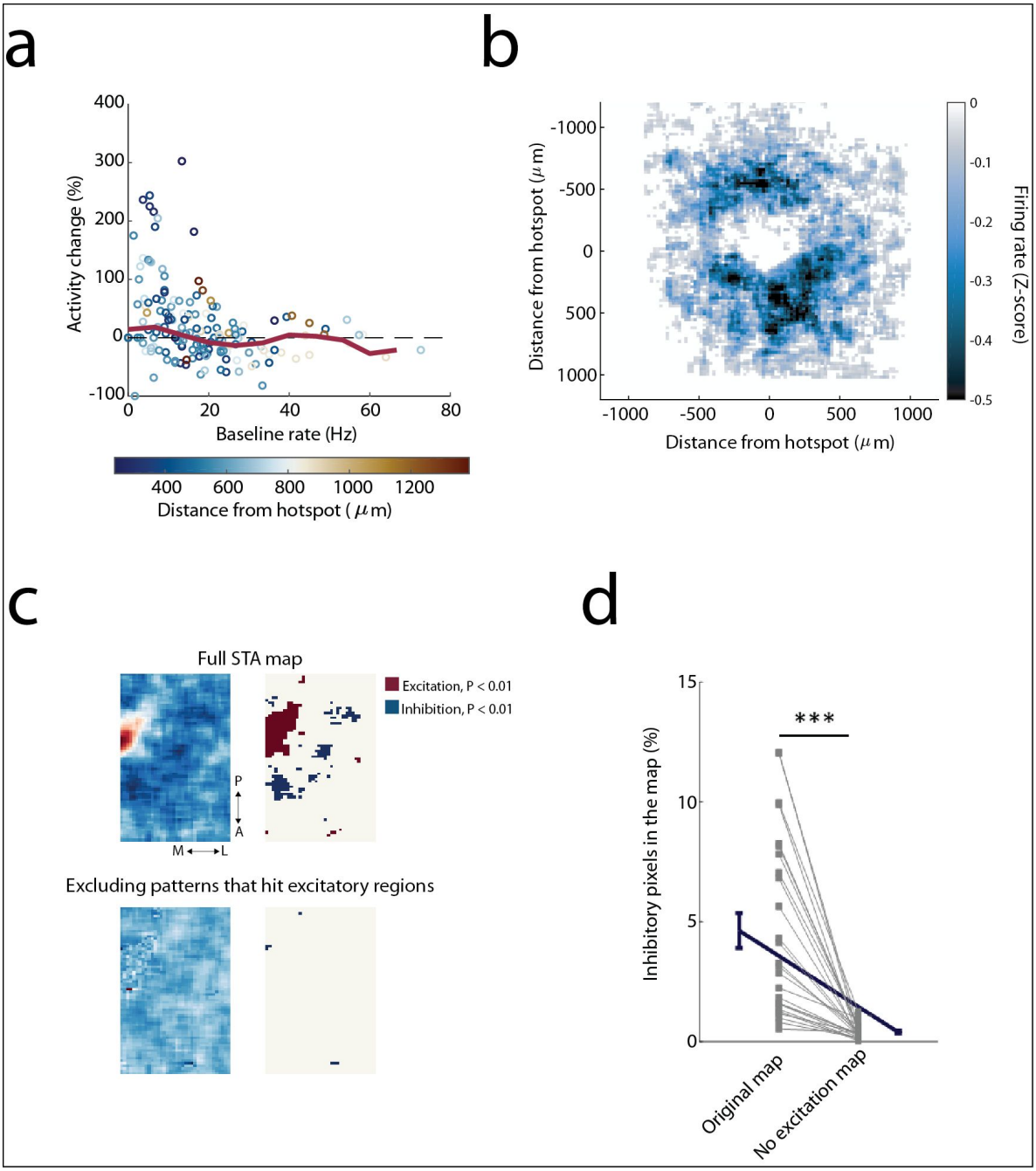

Supplementary Figure 2

MTC lateral suppression is activity- and spatially-dependent

a) Light stimulating a lateral spot without stimulating the hotspot has no effect on the recorded neuron's baseline firing rate, regardless of its firing rates. Color code as in **Figure 2d**.

b) Lateral inhibition is confined in space. All Z-scored STA maps were centered at the hotspot location (N = 27 Z-scored maps, see Methods).

c) MTC lateral suppression is effective only when the target MTC is activated. Upper panels: an example of a MTC receptive field map and the corresponding significance map. Lower panels: the same maps recomputed by excluding all light patterns that stimulated the region around the hotspot (All pixels with significant excitation P < 0.01, relative to shuffled data). No inhibitory regions are detected after exclusion.

d) Population analysis across all MTC STA maps (N = 27) of the percent of inhibitory pixels in the original STA map and when we excluded the light patterns that hit the hotspot area. A pixel is defined as inhibitory if its value is below two standard deviations from the shuffled distribution (see Methods). The percent of inhibitory pixels drops considerably (P = 1.8e-6, two-tailed paired *t*-test), in the excitation-excluded map.

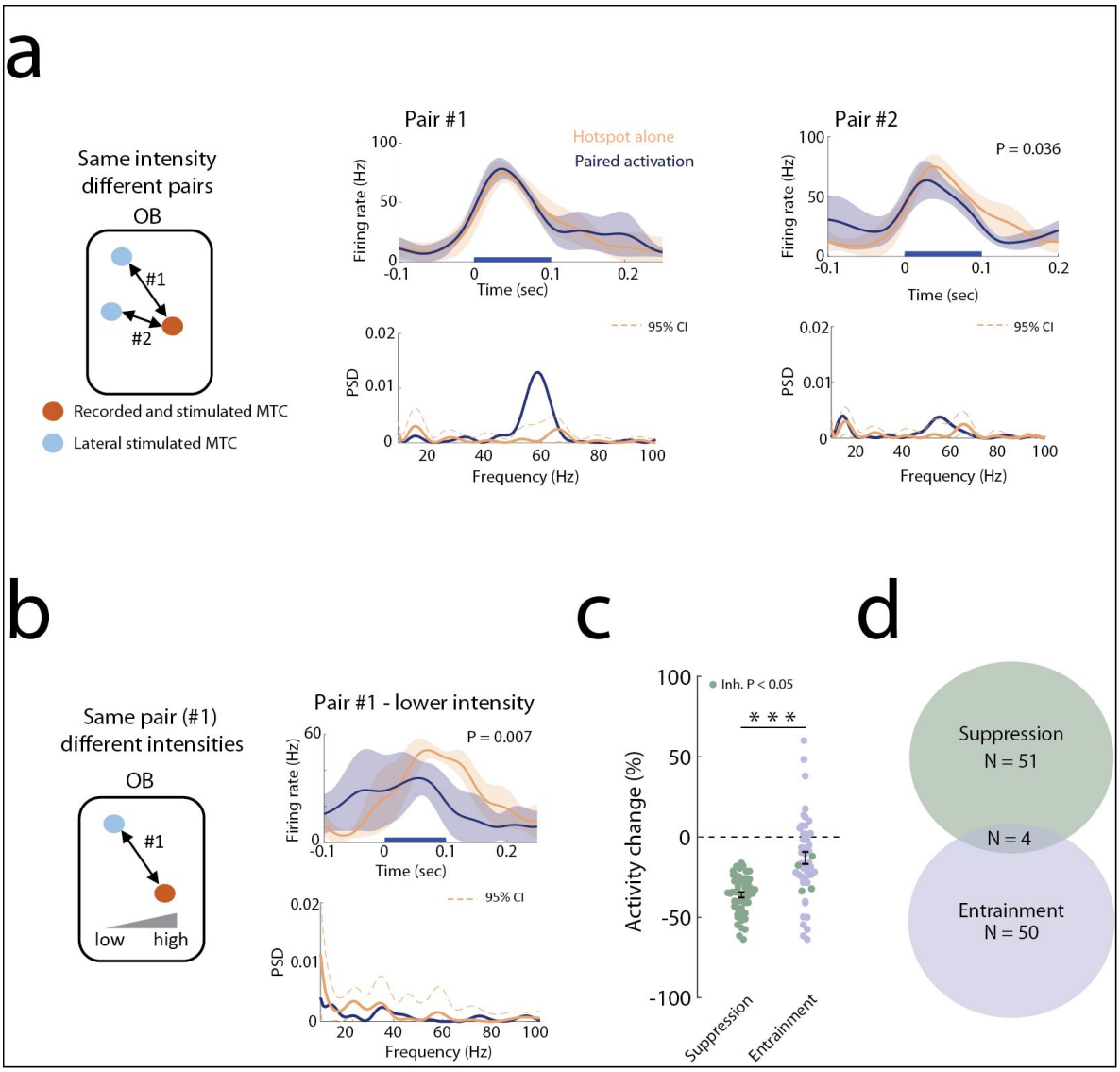

Figure 3

Spike entrainment and suppression are mediated by two different circuits

a) Light stimulation of two different MTC pairs sharing the same postsynaptic MTC. Light-activating of pair #1 (left) caused strong entrainment (P < 0.05, two-sample bootstrap) without affecting the light-evoked firing rate (P = 0.59, two-tailed paired *t*-test), whereas light-activating pair #2 (right) suppressed the MTC firing rate (P = 0.036, two-tailed paired *t*-test), without affecting the spikes precision (P > 0.05, two-sample bootstrap).

b) Two different light intensities were applied to pair #1, which had differential effects on suppression and entrainment. The high light intensity increased spike entrainment without affecting the firing rate (left panel in **a**). In contrast, lower intensity reduced the light-evoked firing rate (P = 0.007, two-tailed paired *t*-test), with no effect on the spikes' gamma entrainment (P > 0.05, two-sample bootstrap).

c) Mean ± SEM of the activity change following paired activation for pairs that evoked significant suppression (green, N = 51) or spike entrainment (purple, N = 50) in the recorded MTC. Both groups significantly differ in their mean activity change (P < 0.001, two-tailed *t*-test, The shared data points were not included in the statistics to allow two independent samples) Green circles in the entrainment group are pairs that evoked both entrainment and spikes suppression of the recorded MTC firing rates (N = 4).

d) A Venn diagram showing a weak overlap between the suppression and entrainment effects.

demonstrated that GCL neurons light-activation increased the recorded MTC spikes' gamma entrainment (**Supplementary Figure 4b-c**). Our results strongly suggest that MTC-to-MTC lateral entrainment is mediated by spatially distributed GCL neurons.

MTC suppression is not mediated by GCL neurons

Finally, we examined how GCL neurons optogenetic activation affects MTC odor-evoked firing rate using the same data from the previous experiment (**Figure 4**). We divided the OB surface into a grid and randomly optogenetically activated GCL neurons columns, with one light spot in each trial of size 330um^2 (**Figure 5a**; N = 31 MTCs). We found that MTC baseline activity was strongly suppressed by light activating GCL neurons, mostly when activating neurons in its vicinity (within its column, **Figure 5a-b**). This experiment validates that in our experimental setup, light stimulation of GCL neurons can suppress MTCs at baseline conditions. In contrast, we found that light-activating sets of GCL neurons during odor stimulation did not change the mean MTC odor-evoked firing rates, irrespective of the MTC firing rate levels. (**Figure 5c**; N = 54 light spots tested from 18 cell-odor pairs, P = 0.64, two-tailed paired *t*-test). To gain insight into whether the change in MTC odor-evoked response depends on the location of the optogenetically activated GCL neurons, we plotted the activity change as a function of the distance from the recorded MTC (N = 54 light spots tested from 18 cell-odor pairs). There was no relationship between the level of suppression and the location of the activated GCL neurons (**Figure 5d**). These findings further suggest that GCL neurons are unlikely to underlie the activity-dependent suppression we observed between MTCs (**Figure 2**). To conclude, our results suggest that MTC-to-MTC lateral entrainment is mediated by spatially distributed GCL neurons, while activity-dependent lateral-suppression, occurs most strongly between adjacent MTCs.

Discussion

Our findings demonstrate two types of interactions between MTCs that shape their firing rate and temporal dynamics. These two interactions are spatially dissociated: Lateral entrainment spans the whole accessible bulb surface, while lateral suppression occurs primarily between adjacent MTCs. Interestingly, both interactions are activity-dependent, with lateral entrainment and lateral suppression peaking when the postsynaptic MTC fires at ~40Hz and ~70-80Hz, respectively. Furthermore, we found that GCL neurons do not mediate substantial MTC-MTC lateral suppression.

MTC and GCL neurons interactions can facilitate the synchronization of co-active and spatially-dispersed MTCs

It has been shown that two active MTCs can synchronize their stimulus-evoked and odor-evoked spike timings (Doucette et al., 2011; Kashiwadani et al., 1999; Schoppa, 2006). However, how this is achieved and how only the odor-activated MTCs are synchronized is unknown. It has been recently hypothesized that GCs may support the synchronization of odor-responding MTCs via activity-dependent mechanism for GABA release (Egger and Kuner, 2021; Lage-Rupprecht et al., 2020). This hypothesis postulates that the spikes of all strongly co-activated MTCs are synchronized to the gamma rhythm, presumably through the GC network. Consistent with this hypothesis, here we have shown that activation of one group of MTCs can increase the spikes entrainment of another, distant, active MTCs, up to one millimeter away. This finding is consistent with a previous study showing distance-independent synchronization between MTCs (Doucette et al., 2011). We found that this increase in synchronization occurred only if the postsynaptic MTC was firing at a certain level (**Figure 1**), suggesting a simple mechanism by which only strongly active MTCs are synchronized.

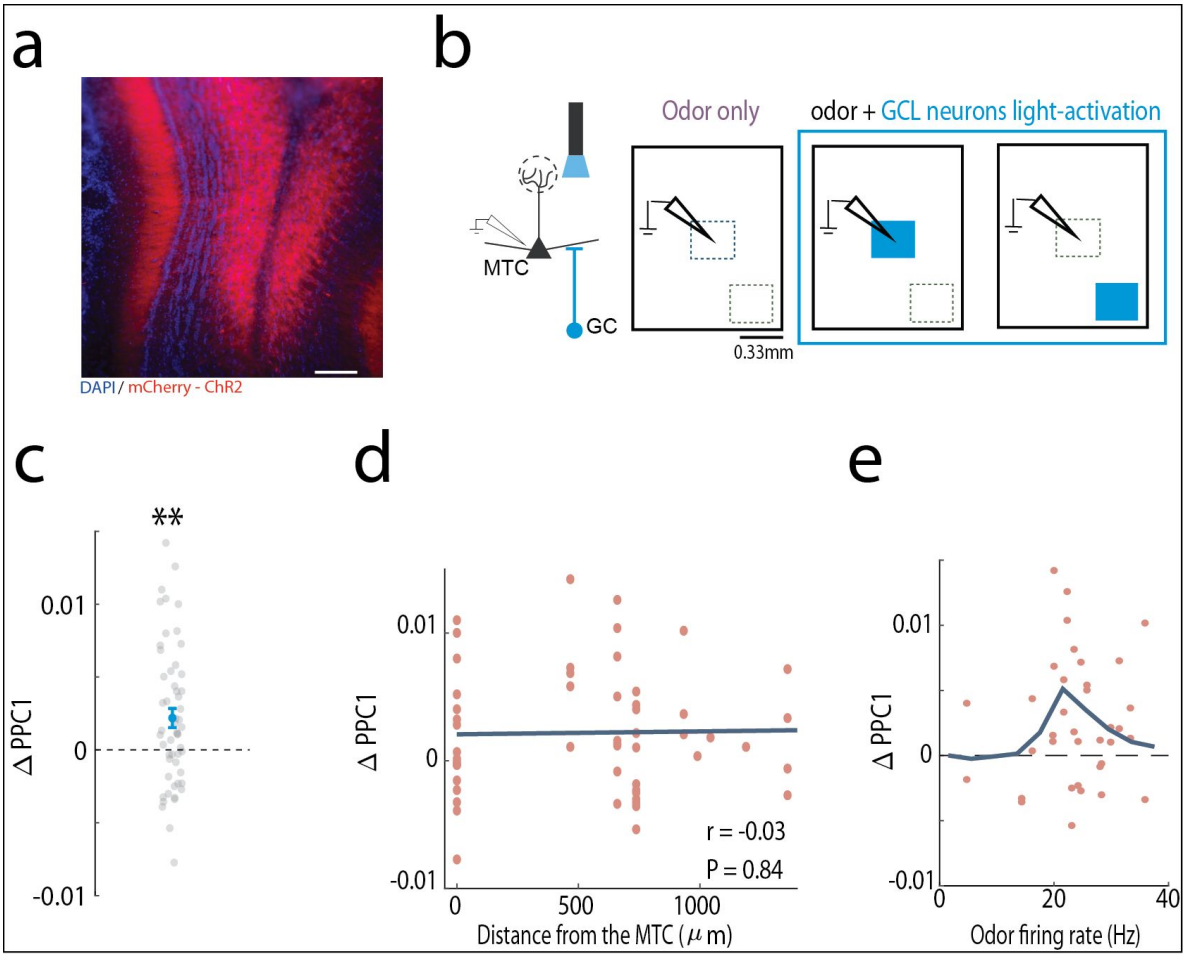

Figure 4

Optogenetic activation of GCL neurons increases MTC synchrony in an activity-dependent and location-independent manner
a) Cre-dependent AAV injected into the GC layer (GCL) of Gad2-Cre mice. A coronal OB section showing restricted ChR2 expression in the GCL and the external plexiform layer, into which GCL neurons extend dendrites (red, mCherry-ChR2; blue, DAPI). Scale bar, 0.1 mm.
b) Schematic illustrations of the experimental setup. Left: Three weeks post injection, MTCs were recorded while light-activating subsets of GCL neurons. Right: MTC activity was recorded in response to odor stimulation alone (purple) or combined with light-activation of GCL neurons near the recording electrode or distant from it (blue). Scale bar, 0.33mm.
c) The change in MTC spike synchrony to the gamma oscillation (L1PPC1) significantly increases under GCL neurons column light-activation during odor stimulation (N = 54, P = 0.0016, two-tailed paired *t*-test). Only cell-odor pairs that were significantly odor-excited were analyzed (N = 18/31 cell-odor pairs; three spots were stimulated per cell odor-pair).
d) MTC spike entrainment does not depend on the location of the light-activated GCL neurons. The relation between the change in PPC1 caused by odor and GCL odor stimulation as a function of the distance of the light-stimulated spot from the recording electrode. No significant correlation was found (N = 54 values from 18 cell-odor pairs, r = -0.03, P = 0.84, Spearman correlation). Zero denotes the spot above the recording electrode.
e) MTC spike entrainment is activity-dependent. The change in synchrony peaked when MTCs fired at ~25Hz.

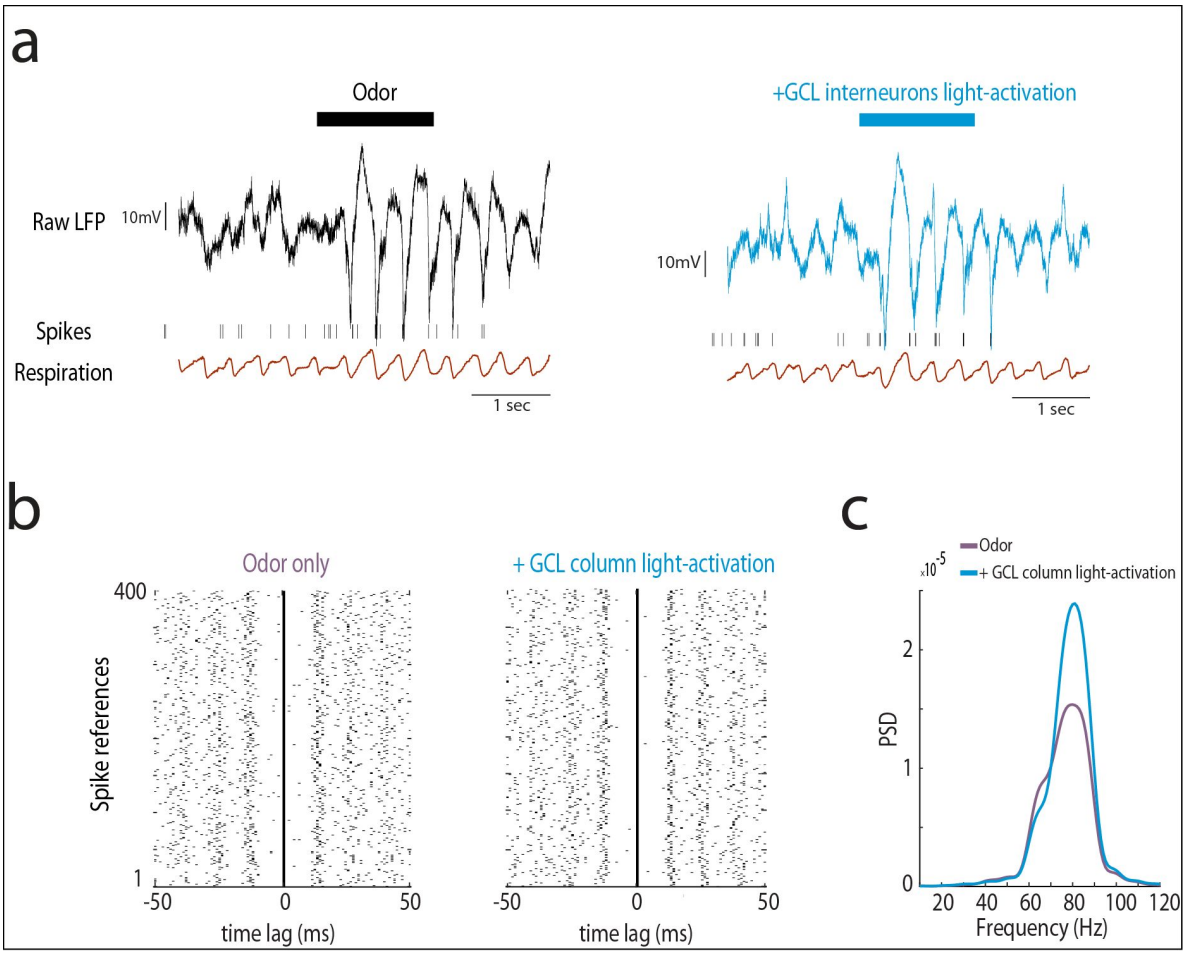

Supplementary Figure 4

Optogenetic activation of GCL neurons increases MTC synchrony in an activity-dependent and location-independent manner
a) Example trials showing the raw LFP data, spike times and respiration signal recorded in response to odor stimulation with and without optogenetic activation of GCL neurons.
b) Odor-evoked spike reference analysis. Two spike raster plots are shown, for odor only (left, purple), and odor with light-activation of a GCL neurons column (right, blue). In each raster plot, spikes are plotted relative to a randomly chosen spike during the odor presentation period (N = 400 spikes references, see Methods). Note the potent spike entrainment when GCL neurons are activated. This analysis was performed on a cell that had a sufficiently high firing rate (see Methods). This cell is likely a tufted cell due to its potent entrainment at the high gamma range, as shown in (Burton and Urban, 2021; Fukunaga et al., 2014).
c) The power spectral densities (PSD) for the two conditions in **b**. A multi-taper analysis of the circular convolution of each spike raster plot was used to compute the PSD (see Methods).

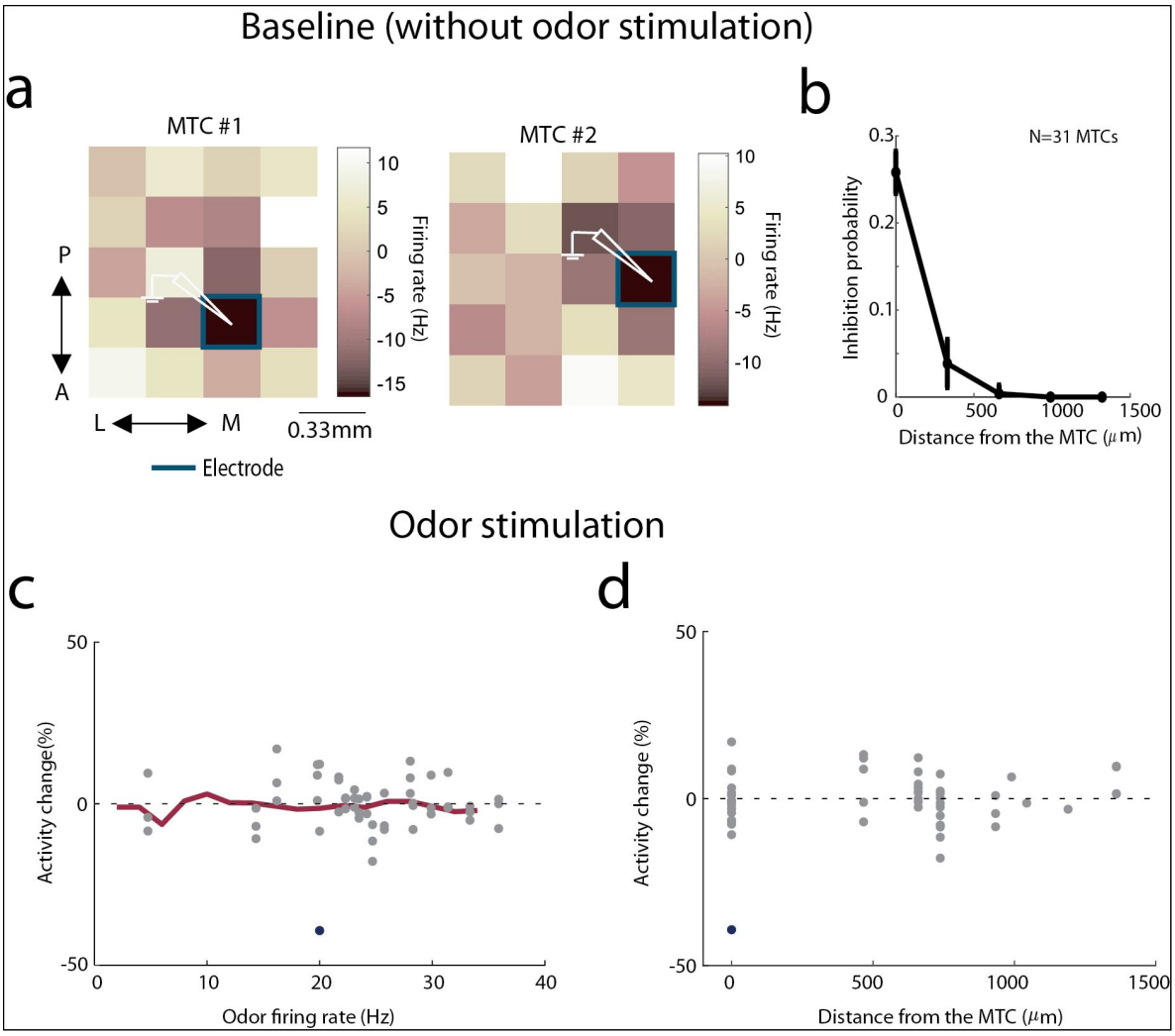

Figure 5

MTC-to-MTC firing rate suppression is not mediated by GCL neurons

a) Shown are OB activity maps from two example MTCs, recorded in different mice, during optogenetic activation of GC-columns at baseline conditions. We divided the OB into a grid and activated light spots of size 330 μm^2. Each entry in the map is color-coded according to the average evoked firing rate across trials. The electrode location is marked by a blue line and a white electrode illustration.

b) A population analysis across all OB activity maps (N = 31 MTCs from 4 mice), showing the probability of obtaining a significant inhibition as a function of the distance from the electrode. MTCs inhibition was restricted to activation of GC-columns in their vicinity.

c) Similar to **Figure 2d**, the change in odor-evoked activity following GC activation is plotted as a function of the recorded MTC odor-evoked firing rates (N = 54 values from 18 cell-odor pairs). Filled blue circles denote significant activity change ($P < 0.05$, two-tailed unpaired *t*-test). A moving average is shown in red.

d) Same data shown as a function of the distance from the electrode. Odor-evoked firing rates are not suppressed when a GC column is activated, irrespective of the GC-optogenetic activation location. Zero marks activation of GCs at the location of electrode.

Lateral suppression is restricted to adjacent and active MTCs

In contrast to the lateral entrainment interactions, we found that lateral suppression of MTC spiking is effective mostly between adjacent MTCs and when the postsynaptic neuron is active at a specific range (~30-80Hz, **Figure 2**). Such lateral suppression properties were theoretically suggested (Cleland and Borthakur, 2020; McIntyre and Cleland, 2016; McTavis et al., 2012) and experimentally validated (Peace et al., 2024). We found that in only ~20% of the tested MTC pairs exhibited significant lateral suppression. This rate is consistent with previous *in-vitro* studies that found lateral suppression between 10-20% of heterotypic MTC pairs (Isaacson and Strowbridge, 1998; Urban and Sakmann, 2002), and is higher compared to a case where the recorded MTC is not active (Lehmann et al., 2016). The role of this lateral suppression, which is most effective when the neurons fire at the gamma range, is unclear. One study suggested that activity-dependent lateral suppression can sharpen MTC odor responses by contrast enhancement (Arevian et al., 2008). However, direct experimental evidence is still lacking.

GCL neurons do not substantially affect MTC odor-evoked firing rates

GCs are the most abundant interneuron type in the OB (Shepherd, 1972), suggesting they have a key role in regulating MTC activity. In line with this hypothesis, several key studies have provided evidence that GCs may suppress the MTC firing rate (Arevian et al., 2008; Giridhar et al., 2011; Yokoi et al., 1995), while later studies demonstrated that EPL interneurons have a key role in suppressing MTC activity (Burton et al., 2024; Huang et al., 2013; Kato et al., 2013). Here, we show that optogenetically activating GC columns during odor stimulation did not substantially affect MTC odor-evoked firing rates. Although this contradicts a previous in-vitro result (Arevian et al., 2008), it is consistent with a recent in-vivo study that found no increase in MTC firing rates when silencing GC activity either in anesthetized or in awake mice (Fukunaga et al., 2014). It is worth noting that light-activating large numbers of GCs can suppress MTC odor-evoked responses (Dalal and Haddad, 2022; Gschwend et al., 2015). However, activation of all GCL neurons is unlikely to occur during natural odor response. We speculate that MTC-to-MTC suppression is mediated by EPL neurons, most likely the Parvalbumin neuron (PV). This hypothesis is based on their activity and connectivity properties with MTCs (Burton, 2017; Burton et al., 2024b; Guest et al., 2021; Huang et al., 2013; Kato et al., 2013; Miyamichi et al., 2013). Of note, it is possible that our viral transfection protocol in Gad2-Cre mice might not transfected all subtypes of GCs, which may explain the lack of substantial suppressive effect onto MTCs. Future studies are required to shed light on how PV neurons affect MTC activity.

MTC-GCL neurons interactions under anesthesia

Our experiments were performed under Ketamine anesthesia, an NMDA receptor antagonist that affects the reciprocal dendro-dendritic synapses between MTCs and GCs (Egger and Kuner, 2021; Lage-Rupprecht et al., 2020). Consistent with that, recent studies reported lower GC excitability under anesthesia (Cazakoff et al., 2014; Kato et al., 2012). This raises the concern that our result might not be valid in the awake state. We argue that this is unlikely. First, (Fukunaga et al., 2014) reported that GCs baseline activity in anesthetized and awake mice is similar, suggesting that MTC-GC synapses function. Second, we show that light activation of GCL neurons strongly inhibits the MTC baseline activity (**Figure 5**) and increases MTC odor-evoked spike-LFP coupling in the gamma range (**Figure 4**). These experiments validate that GCL neurons can exert inhibition over MTCs in our experimental setup. Third, we have shown that light-activating all accessible GCL neurons has a minor effect on the MTC odor-evoked firing rates in an awake state (Dalal and Haddad, 2022), corroborating the finding that GCL neurons are unlikely to provide strong suppression to MTCs. Fourth, and most importantly, we showed that optogenetic stimulation of MTCs entrains other MTC spike times, which is achieved via the GCL neurons. This suggests that the lack of lateral suppression following MTC or GCL neuron opto-

activation is not due to MTC-GC synapse blockage. That said, we cannot exclude the unlikely possibility that NMDA receptor blockage under anesthesia impairs MTC-to-MTC suppressive interactions but not the MTC-to-MTC mediated spike entrainment.

Downstream integration of synchronous MTC activity

How do downstream olfactory cortex neurons benefit from synchronous MTC activity? Anterior piriform cortex (aPC) neurons integrate the activity of several active MTCs and act as coincidence detectors (Davison and Ehlers, 2011; Haddad et al., 2013). Recently, we have shown that increased MTC spike phase-locking to OB gamma oscillations enhanced aPC neurons' odor representation (Dalal and Haddad, 2022). This current study extends these findings as it demonstrates that the co-activation of MTCs increases their spikes' gamma entrainment. Moreover, this lateral synchronization is mediated via the GC network. In summary, we found that MTC interactions shape odor-evoked MTC firing rates and spike times. Both of these changes are activity-dependent. Activity-dependent synchronization can enable the synchronization of odor-activated MTCs dispersed across the glomerular map. Since glomeruli columns are zero-phase synchronized (Peace et al., 2024), and the odor-activated MTCs are synchronized to the same phase (Doucette et al., 2011; Kashiwadani et al., 1999), the efficacy of odor information transform to downstream neurons will increase (Dalal and Haddad, 2022). Moreover, activity-dependent spike suppression might enhance odor representation in the OB by reducing low and noisy odor-evoked MTC responses. Finally, our findings suggest that two types of OB interneurons mediate these distinct interactions.

Acknowledgements

This study was supported by a grant from the Israel Science Foundation ICORE program [11/51].

Additional information

Author contributions

T.D. performed the experiments and analyzed the data, T.D. and R.H conceptualized the experiments and wrote the paper.

Competing Interest Statement

The authors declare no conflict of interest.

Methods

All surgical and experimental procedures were conducted in accordance with the National Institutes of Health Guide for the Care and Use of Laboratory Animals and Bar Ilan University guidelines for the use and care of laboratory animals in research, and were approved and supervised by the Institutional Animal Care and Use Committee (IACUC). Animals were housed in a group cage and received no experimental treatment, except genotyping. The animals were maintained in a reverse light/dark cycle, and all experiments were performed during the dark period. 19 Tbet-Cre (Jackson Laboratory, Stock No. 024507) crossed with Ai32 (Jackson Laboratory, Stock No. 012569), and 4 Gad2-ires-Cre (Jackson Laboratory, Stock No. 028867) male and female mice aged 3-12 months were used. As no differences in light-evoked responses were observed between sexes, data from both sexes was pooled.

Surgical Procedures for Electrophysiology Recordings

Animals were anesthetized with ketamine/ medetomidine (60/ 0.5 mg/ kg, i.p.) and then fixed in a stereotaxic frame. The bone overlaying the dorsal OBs was removed. Additional anesthesia was administered as needed (~30% of the original dose of ketamine/ medetomidine). Body temperature was maintained at 36-37°C using a homoeothermic blanket system (Harvard Apparatus).

Viral Injections

Mice were briefly anesthetized with isoflurane before an intraperitoneal injection of ketamine/ medetomidine (60/ 0.5 mg/ kg i.p.). The mouse was head-fixed in a stereotaxic frame, and AAV5-EF1a-DIO-ChR2-eYFP/mCherry (titers: 4×10^{12} particles/ ml; University of North Carolina Gene Therapy Center) was injected into the granule cell layer. To infect GCL neurons, we modified an injection protocol employing five injection sites in two tracks, as reported elsewhere (Fukunaga et al., 2014). The coordinates for the first track were +0.9 mm (M-L) from the midline rhinal fissure, +0.8 mm (A-P), and three sites at the D-V axis at -0.8 mm (300 nl), -1.1 mm (200 nl), and -1.3 mm (200 nl). Second track coordinates were +0.9 mm (M-L) from the midline rhinal fissure, +1.2 mm (A-P) and 2 sites at the D-V axis at -0.8 mm (200 nl), and -1.1 mm (200 nl). M-L coordinates are relative to the midline rhinal fissure. The syringe was left in place for at least three minutes before moving to the next coordinate on the D-V axis. The virus was injected using a micro-injector (IMS-10, Narishige, Japan) at a rate of 70 nl/ min, which was left in place for 5 minutes to allow viral particle diffusion before needle removal. Incisions were closed with tissue glue (Vetbond), and an analgesic injection (Carprofen) was administered at the end of the surgery. Electrophysiology was carried out at least three weeks post-viral injection.

Electrophysiology

The neurons' extracellular activity and local-field potential (LFP) were recorded using tungsten electrodes (~1-10 MΩ; FHC). Neural signals were amplified and first filtered at 1-10,000Hz and then at 300-5,000 Hz for spiking activity (AM-Systems 1800), sampled, and recorded at 40 kHz (National Instruments, Austin, TX). Spike signals were sorted offline using MClust software in MATLAB (written by A.D. Redish, University of Minnesota). MTC recordings were collected from the dorsal OB (~200-500 μm). The electrode was typically lowered at an angle of 90 degrees. The depth of recorded neurons was estimated when the recording electrode was withdrawn using a micromanipulator.

Optogenetic Stimulation of the Olfactory Bulb

Optogenetic stimulation of neurons in the OB was performed using an optical imaging system based on a digital micro-mirror (OPTOMA X600 DLP Projector), as described in (Grobman et al., 2018). Precise spatial control of optical stimulation was achieved by projecting two-dimensional light patterns over the dorsal surface of the OB. We used blue and white light for MTC and GC activation, respectively. For MTC stimulation (Tbet-Cre mice crossed with Ai32 mice), a blue filter was placed on top of the collimating lens, which was placed at a distance of ~20 cm from the projector (f = 75 mm, Achromatic doublets, Thorlabs). This configuration resulted in an image where each projected pixel corresponded to a square of 22 μm^2. The size of the craniotomy determined the light stimulation boundaries of each experiment. Optical stimulation was controlled with the MATLAB psychophysical toolbox. We used a photodiode (FDS1010, 400-ns rise time, Thorlabs) to obtain a timestamp for each light stimulus. The light intensity ranged between ~0.1-~1.5 mW/ mm^2 as measured with an optical power meter (Thorlabs PM100D). The stimulation frequency of the optical imaging system was 120 Hz.

Spike-Triggered Average (STA)

The spike-triggered average calculation was described previously by (Grobman et al., 2018). Briefly, STA was used to characterize the receptive field of the recorded MTC. Here, we use the term 'receptive field' in a more abstract sense to refer to the ensemble of all neurons on the bulb's surface that modify the recorded neuron activity.

We stimulated the dorsal OB with patterns of multiple square spots measuring 88-110 μm^2. Light spots within a pattern could overlap up to a shift of one pixel (22μm). The stimuli duration was 0.1 sec, and the inter-stimuli-interval between consecutive patterns ranged between 0.1-0.2 sec. The number of spots projected in each trial ranged between 5-10, and the number of trials per recording ranged between 2000-3000. We computed the response map for each cell by computing the spike-triggered average, which is the weighted firing rate average of all projected stimuli.

$$STA = \frac{\sum_{i=1}^{N} P_i R_i}{\sum_{i=1}^{N} R_i}$$

P_i is the 2-dimensional projected light pattern, and R_i is the evoked firing rate following stimulus P_i.

Paired light stimulation

Single light spots (over the hotspot or a lateral spot) or paired stimulation (both together) of size ~154 μm^2 were projected at varying light intensities (range ~0.1 to ~1.5 mW/ mm^2, reported in **Figures 1**-**3**). Spots were selected either randomly or manually. In the manual selection case, we selected spots that caused either significant or mild but insignificant inhibitory effects on the recorded MTC (e.g., local cold spots in the receptive-field map; see example in **Figure 2a** of example spots that were selected manually). The number of trials for each condition at a given light intensity was 15, and the inter-stimuli interval (ISI) was set to 1.5 seconds.

Optogenetic activation of GCL neurons during baseline and odor stimulation

To verify the effect of optogenetic activation of GCL neurons on the recorded MTC, we scanned the OB with light spots, without stimulating the MTC. Light spots were of size 330μm^2, each spot was illuminated 20-30 times, the light duration was 0.2 sec, and the ISI was 0.4 sec. The light intensity was as described in (Dalal & Haddad 2022). As expected, we found a 'coldspot' (i.e. a reduction in firing rate) in the vicinity of the electrode location (**Figure 5**), confirming that light-activating GCL neurons evokes robust inhibition to reduce MTC baseline activity, consistent with a recent study (Huang et al., 2016). For optogenetic activation of GCL neurons during odor stimulation, the odor duration was 1.5 seconds. The light stimulus was active throughout the odor stimulation period. The activation of GCL neurons at different locations during odor stimulation was performed based on the activity map generated under baseline conditions. In each of the three conditions in this experiment, odor stimulation alone or combined with GCL neurons column activation, the number of trials was at least 10, with an ISI of 10-15 seconds. In these experiments, the LFP was simultaneously recorded using the same electrode, and the signal was later filtered for spiking activity (300-5000 Hz) and LFP ranges (1-300 Hz).

Respiration Analysis

We recorded the respiration signal using a piezoelectric sensor (APS4812B-LW100-R, PUI Audio). The most salient feature of the respiratory signal is the peak in the middle of the inhalation cycle caused by the pressure of the diaphragm on the sensor. The onsets of inhalation and exhalation were defined as the zero-crossings of the signal before and after the peak, respectively.

Odorant Application

Odorants were applied using a custom-built olfactometer. Odorants were diluted in mineral oil (1:100) and stored in sealed glass vials. This concentration was chosen to elicit a detectable response. The tubes were placed in front of the animals' nostrils at a distance of ~2 cm. Airflow was controlled with a mass flow controller (Agilent, Alimc-2LSPM) and set to 0.8 slpm. Air circulated freely between stimulations to reduce odorant remnants. A vent removed residual odorants. Odorant stimulation times and sequences were controlled by custom MATLAB scripts. The odorant stimulation time was set to 1.5 sec., with an inter-trial interval of 10-15 sec. The odorant sequence was randomized, and each stimulus was delivered at least ten times. All odorants used (all at 1% dilution) were from Sigma-Aldrich at their highest purity. The odorants used were Phenethylamine (PEA (CAS: 64-41-0), Ethyl acetate (CAS: 141-78-6), Ethyl valerate (CAS: 539-82-2), 2-heptanone (CAS: 110-43-0), Ethyl butyrate (CAS: 105-54-4), Ethyl tiglate (CAS: 5837-78-5), and Acetophenone (CAS: 98-86-2).

Quantification and statistical analysis

General Statistical Analysis

All data analyses were performed in MATLAB. The figures or figure legends detail the number of data points used for all statistical tests and graphs. Significance alpha was defined as a 0.05/0.01. Unless stated otherwise, we report the mean ± SEM or %95 confidence interval. Mean ± standard deviation is reported when estimated from a bootstrap process. We used a *t*-test as required by the test's null hypothesis and population assumptions. All tests were two-tailed. The test is reported in the figure legend or the main text.

Data Analysis Spike Sorting

Spike signals were sorted and clustered offline using MClust software in MATLAB (written by A.D. Redish) or Spike3D (Neuralynx). Only visually well-isolated clusters were used, with less than 5% of spikes violating an inter-spike interval of 2 ms.

Significant regions in the STA map

Computation of significant activity change of each pixel of the STA map was done relative to a shuffled STA map. The shuffled map was generated by shuffling the patterns indices and computing the shuffled STA (multiplying the shuffled patterns with the original firing rate as described above). Then, the 0.5 and 99.5 percentile values from the shuffled map were determined. The values in the STA map that were above or below these high and low percentile thresholds were assigned as significant excitatory and inhibitory pixels, respectively.

Superimposed STA maps

To analyze the spatial location of the inhibitory regions surrounding the recorded MTC, each STA map was Z-scored using the mean and standard deviation values on the map. We then thresholded the map such that only pixels with a Z-score <= -1 remained. The hotspot peak was centered at the origin, and the inhibition values were plotted on the map relative to the hotspot. We superimposed all maps and averaged across all neurons. We computed the radial average of this map by averaging all angles from the center of the map.

Exclusion of excitatory regions in STA maps

STA maps were recomputed by excluding trials with at least one light spot that hit the significant excitatory regions in the map. The significance of each pixel in the recomputed map was registered, and the percent of inhibitory pixels in the original and recomputed map was assigned. To verify that the lower number of significant pixels in the recomputed map was not due to a smaller number of trials, for each full map we randomized the same number of trials that were used to construct the recomputed map and computed the STA. We found no significant change in the percent of inhibitory spots compared with the original map (data not shown).

Quantification of MTC lateral inhibition

A pair of light-stimulated MTCs was considered as evoking lateral inhibition if it met two criteria: the response to the hotspot stimulation was significantly different from baseline ($P < 0.05$, one-tailed paired *t*-test), and there was a significant change in the firing rate across trials between hotspot stimulation and paired activation within a window of 200 ms ($P < 0.05$, two-tailed unpaired *t*-test, stimulus duration 100 ms). A window of 200 ms was used to account for neural responses with a slower return to baseline. The distance between the spots in the pair was measured using Euclidean distance. The activity change measure was defined as:

$$100\ X\ \frac{mean(paired\ activation\ firing\ rate) - mean(hotspot\ firing\ rate)}{mean(hotspot\ firing\ rate)}$$

MTC entrainment across trials

Quantifying MTC spike entrainment across trials was done by computing the PSTH of each condition during the light period (100 ms) using a Gaussian kernel with a standard deviation of 2 ms. The PSTHs were zero-padded to a length of 1 second, Z-scored, and the power spectrum density was computed using multi-taper analysis (TW = 3 Hz, L = (2*TW)-1, where L is the number of orthogonal Slepian tapers). The change in entrainment measure was the difference between the integral of paired activation and the hotspot alone at 40-70 Hz. We analyzed only pairs and light intensities that significantly responded to light stimulation ($P < 0.05$, two-tailed paired *t*-test). Shuffled distribution of spike entrainment was obtained by shuffling the trial identities and computing the power spectrum density integral difference. The differential entrainment values were labeled significant if they crossed the 95% confidence interval around the shuffled distribution.

Time-Frequency Analyses of MTC entrainment

Time-frequency representation was performed using the continuous wavelet transform (the analytic 'Morse' wavelet, 8 octaves, 32 voices per octave; MathWorks) over the Peri-stimulus time histograms (PSTH) across trials (Gaussian window of 2 ms standard deviation).

Odor-Evoked Responses

An odor firing rate was computed over the first two seconds following odor presentation. This time window included an additional 0.5 sec after stimulus offset to account for neural responses with a slower return to baseline. Trials were aligned to odor onset so that the analyzed neural activity would be aligned with the light stimulation. A response was defined as significant if the firing rate was significantly different from the average firing rate over an equivalent time window prior to stimulus onset ($P < 0.05$, two-tailed paired *t*-test). PSTHs were smoothed using a Gaussian filter (standard deviation of 50 ms, Chronux toolbox).

LFP Analysis

Recorded LFP signals were down-sampled to 4 kHz and band-pass filtered to the γ-band frequency range (40-70 Hz) using the MATLAB (MathWorks) filter designer (Butterworth IIR filter with order 1). The line noise (50 Hz) was filtered using an IIR bandstop filter (48-52 Hz). We focused our analysis on the low γ-band frequency range as a prominent oscillation in this range in the olfactory bulb was previously reported (Cenier et al., 2009; Lepousez and Lledo, 2013).

Spikes-LFP pairwise phase consistency (PPC)

Spike-LFP coupling was computed using the pairwise phase consistency 1 (PPC1) measure (Vinck et al., 2012, 2013). For each neuron, we extracted the spike phases from all trials. To compute the spike phases per trial, we extracted the instantaneous phase of the corresponding γ-band-filtered LFP (40-70 Hz) using the Hilbert transform, assigned a phase to each spike (0–2π) and pooled the phases across all trials. The PPC1 values were the mean dot-product of all pairwise spike phases, excluding phases of spikes from the same trial.

Spike reference analysis

We performed a spike reference analysis to quantify the entrainment of odor-evoked MTC spikes, as seen elsewhere (Fukunaga et al., 2014). Spike reference raster plots were constructed for each condition by randomizing 400 spikes from all trials that occurred at a time window of 1 second after odor onset. Each randomized spike served as a reference and was set to time lag 0, and the spikes in a window of ± 50 ms around it were plotted relative to the reference. Choosing a different number of randomized spikes or a different window size did not affect the results. We then computed the PSTH of the raster plot, subtracted its mean, and performed a circular convolution. To compute the power spectral density of the raster plot, we zero-padded the convolved signal into one 1-second length and applied a multi-taper analysis (TW = 5 Hz). The PSD curve was smoothed using a rectangular window of order 15.

References

Arevian A.C., Kapoor V., Urban N.N (2008) **Activity-dependent gating of lateral inhibition in the mouse olfactory bulb** *Nat Neurosci* **11**:80–87

Beshel J., Kopell N., Kay L.M (2007) **Olfactory bulb gamma oscillations are enhanced with task demands** *J. Neurosci* **27**:8358–8365

Burton S.D (2017) **Inhibitory circuits of the mammalian main olfactory bulb** *J. Neurophysiol* **118**:2034–2051

Burton S.D., Urban N.N (2021) **Cell and circuit origins of fast network oscillations in the mammalian main olfactory bulb** *Elife* **10**:1–29

Burton S.D., Malyshko C.M., Urban N.N (2024) **Fast-spiking interneuron detonation drives high-fidelity inhibition in the olfactory bulb** *PLOS Biol* **22**

Burton S.D., Malyshko C.M., Urban N.N (2024) **Fast-spiking interneuron detonation drives high-fidelity inhibition in the olfactory bulb** *BioRxiv*

Buzsáki G (2010) **Neural Syntax: Cell Assemblies, Synapsembles, and Readers** *Neuron* **68**:362–385

Buzsáki G., Chrobak J.J (1995) **Temporal structure in spatially organized neuronal ensembles: a role for interneuronal networks** *Curr. Opin. Neurobiol* **5**:504–510

Cazakoff B.N., Lau B.Y.B., Crump K.L., Demmer H.S., Shea S.D (2014) **Broadly tuned and respiration-independent inhibition in the olfactory bulb of awake mice** *Nat. Neurosci* **17**:569–576

Cenier T., François D., Philippe L., Samuel G., Corine A., Nathalie B (2009) **Respiration-gated formation of gamma and beta neural assemblies in the mammalian olfactory bulb** *Eur. J. Neurosci* **29**:921–930

Cleland T.A., Borthakur A (2020) **A Systematic Framework for Olfactory Bulb Signal Transformations** *Front. Comput. Neurosci* **14**:1–15

Dalal T., Haddad R (2022) **Upstream γ-synchronization enhances odor processing in downstream neurons** *Cell Rep* **39**

Davison I.G., Ehlers M.D (2011) **Neural circuit mechanisms for pattern detection and feature combination in olfactory cortex** *Neuron* **70**:82–94

Doucette W., Gire D.H., Whitesell J., Carmean V., Lucero M.T., Restrepo D (2011) **Associative cortex features in the first olfactory brain relay station** *Neuron* **69**:1176–1187

Egger V., Kuner T (2021) **Olfactory bulb granule cells: specialized to link coactive glomerular columns for percept generation and discrimination of odors** *Cell Tissue Res* **383**:495–506

Egger V., Urban N.N (2006) **Dynamic connectivity in the mitral cell-granule cell microcircuit** *Semin. Cell Dev. Biol* **17**:424–432

Fantana A.L., Soucy E.R., Meister M (2008) **Rat olfactory bulb mitral cells receive sparse glomerular inputs** *Neuron* **59**:802–814

Fukunaga I., Herb J.T., Kollo M., Boyden E.S., Schaefer A.T (2014) **Independent control of gamma and theta activity by distinct interneuron networks in the olfactory bulb** *Nat. Neurosci* **17**:1208–1216

Galán R.F., Fourcaud-Trocmé N., Ermentrout G.B., Urban N.N. (2006) **Correlation-induced synchronization of oscillations in olfactory bulb neurons** *J. Neurosci* **26**:3646–3655

Giridhar S., Doiron B., Urban N.N (2011) **Timescale-dependent shaping of correlation by olfactory bulb lateral inhibition** *Proc Natl Acad Sci U S A* **108**:5843–5848

Grobman M., Dalal T., Lavian H., Shmuel R., Belelovsky K., Xu F., Korngreen A., Haddad R (2018) **A Mirror-Symmetric Excitatory Link Coordinates Odor Maps across Olfactory Bulbs and Enables Odor Perceptual Unity** *Neuron* **99**:800–813

Gschwend O., Abraham N.M., Lagier S., Begnaud F., Rodriguez I., Carleton A (2015) **Neuronal pattern separation in the olfactory bulb improves odor discrimination learning** *Nat. Neurosci* **18**:1474–1482

Guest C. *et al.* (2021) **Feasibility of integrating canine olfaction with chemical and microbial profiling of urine to detect lethal prostate cancer** *PLoS One* **16**:1–23

Haddad R., Lanjuin A., Madisen L., Zeng H., Murthy V.N., Uchida N (2013) **Olfactory cortical neurons read out a relative time code in the olfactory bulb** *Nat. Neurosci* **16**:949–957

Huang L., Garcia I., Jen H.I., Arenkiel B.R (2013) **Reciprocal connectivity between mitral cells and external plexiform layer interneurons in the mouse olfactory bulb** *Front Neural Circuits* **7**

Huang X.L., Ung K., Garcia I., Quast K.B., Cordiner K., Saggau X., Arenkiel X.B.R (2016) **Task Learning Promotes Plasticity of Interneuron Connectivity Maps in the Olfactory Bulb** *J Neurosci.* **36**:8856–8871

Isaacson J.S., Strowbridge B.W (1998) **Olfactory reciprocal synapses: dendritic signaling in the CNS** *Neuron* **20**:749–761

Kashiwadani H., Sasaki Y.F., Uchida N., Mori K (1999) **Synchronized oscillatory discharges of mitral/tufted cells with different molecular receptive ranges in the rabbit olfactory bulb** *J. Neurophysiol* **82**:1786–1792

Kato H.K., Chu M.W., Isaacson J.S., Komiyama T (2012) **Dynamic Sensory Representations in the Olfactory Bulb: Modulation by Wakefulness and Experience** *Neuron* **76**:962–975

Kato H.K., Gillet S.N., Peters A.J., Isaacson J.S., Komiyama T (2013) **Parvalbumin-Expressing Interneurons Linearly Control Olfactory Bulb Output** *Neuron*

Lage-Rupprecht V., Zhou L., Bianchini G., Aghvami S.S., Mueller M., Rózsa B., Sassoè-Pognetto M., Egger V. (2020) **Presynaptic nmdars cooperate with local spikes toward gaba release from the reciprocal olfactory bulb granule cell spine** *Elife* **9**:1–27

Lehmann A., D'Errico A., Vogel M., Spors H (2016) **Spatio-Temporal Characteristics of Inhibition Mapped by Optical Stimulation in Mouse Olfactory Bulb** *Front. Neural Circuits* **10**

Lepousez G., Lledo P.M (2013) **Odor Discrimination Requires Proper Olfactory Fast Oscillations in Awake Mice** *Neuron*

Macleod K., Laurent G., Ba A (1998) **Who reads temrpoal information contained across synchonized and oscillatory spike trains?** *Nature* **395**:693–698

McIntyre A.B.R., Cleland T.A (2016) **Biophysical constraints on lateral inhibition in the olfactory bulb** *J. Neurophysiol* **115**

McTavis T.S., Migliore M., Shepherd G.M., Hines M.L (2012) **Mitral cell spike synchrony modulated by dendrodendritic synapse location** *Front. Comput. Neurosci* **6**:1–12

Miyamichi K., Shlomai-Fuchs Y., Shu M., Weissbourd B.C., Luo L., Mizrahi A (2013) **Dissecting local circuits: Parvalbumin interneurons underlie broad feedback control of olfactory bulb output** *Neuron* **80**:1232–1245

Peace S.T., Johnson B.C., Werth J.C., Li G., Kaiser M.E., Fukunaga I., Schaefer A.T., Molnar A.C., Cleland T.A (2024) **Coherent olfactory bulb gamma oscillations arise from coupling independent columnar oscillators** *J. Neurophysiol* **131**:492–508

Pressler R.T., Strowbridge B.W (2017) **Direct Recording of Dendrodendritic Excitation in the Olfactory Bulb : Divergent Properties of Local and External Glutamatergic Inputs Govern Synaptic** *Integration in Granule Cells* **37**:11774–11788

Pritchett D.L., Siegle J.H., Deister C.A., Moore C.I (2015) **For things needing your attention: The role of neocortical gamma in sensory perception** *Curr. Opin. Neurobiol* **31**:254–263

Schoppa N.E (2006) **Synchronization of olfactory bulb mitral cells by precisely timed inhibitory inputs** *Neuron* **49**:271–283

Shepherd G.M (2004) **The synaptic organization of the brain** Oxford University Press

Sohal V.S. (2016) **How close are we to understanding what (If anything) γ oscillations do in cortical circuits?** *J. Neurosci.* **36**:10489–10495

Urban N.N., Sakmann B (2002) **Reciprocal intraglomerular excitation and intra- and interglomerular lateral inhibition between mouse olfactory bulb mitral cells** *J. Physiol* **542**:355–367

Vinck M., Battaglia F.P., Womelsdorf T., Pennartz C (2012) **Improved measures of phase-coupling between spikes and the Local Field Potential** *J. Comput. Neurosci* **33**:53–75

Vinck M., Womelsdorf T., Buffalo E.A., Desimone R., Fries P (2013) **Attentional Modulation of Cell-Class-Specific Gamma-Band Synchronization in Awake Monkey Area V4** *Neuron* **80**:1077–1089

Yokoi M., Mori K., Nakanishi S (1995) **Refinement of odor molecule tuning by dendrodendritic synaptic inhibition in the olfactory bulb** *Proc Natl Acad Sci U S A* **92**:3371–3375

Author information

Tal Dalal
The Gonda Multidisciplinary Brain Research Center, Bar-Ilan University, Ramat-Gan, Israel

Rafi Haddad
The Gonda Multidisciplinary Brain Research Center, Bar-Ilan University, Ramat-Gan, Israel
ORCID iD: 0000-0001-8285-5210

For correspondence: rafi.haddad@biu.ac.il

Editors

Reviewing Editor
Nicolás Pírez
Universidad de Buenos Aires - CONICET, Buenos Aires, Argentina

Senior Editor
Laura Colgin
University of Texas at Austin, Austin, United States of America

Reviewer #1 (Public review):

Summary:

Dalal and Haddad investigated how neurons in the olfactory bulb are synchronized in oscillatory rhythms at gamma frequency. Temporal coordination of action potentials fired by projection neurons can facilitate information transmission to downstream areas. In a previous paper (Dalal and Haddad 2022, https://doi.org/10.1016/j.celrep.2022.110693), the authors showed that gamma frequency synchronization of mitral/tufted cells (MTCs) in the olfactory bulb enhances the response in the piriform cortex. The present study builds on these findings and takes a closer look at how gamma synchronization is restricted to a specific subset of MTCs in the olfactory bulb. They combined odor and optogenetic stimulations in anesthetized mice with extracellular recordings.

The main findings are that lateral synchronization of MTCs at gamma frequency is mediated by granule cells (GCs), independent of the spatial distance, and strongest for MTCs with firing rates close to 40 Hz. The authors conclude that this reveals a simple mechanism by which spatially distributed neurons can form a synchronized ensemble. In contrast to lateral synchronization, they found no evidence for the involvement of GCs in lateral inhibition of nearby MTCs.

Strengths:

Investigating the mechanisms of rhythmic synchronization in vivo is difficult because of experimental limitations for the readout and manipulation of neuronal populations at fast timescales. Using spatially patterned light stimulation of opsin-expressing neurons in combination with extracellular recordings is an elegant approach. The paper provides evidence for an activity-dependent synchronization of MTCs in gamma frequency that is mediated by GCs.

Weaknesses:

The study provides several results showing the firing of MTCs in gamma frequency range, however, direct evidence for the synchronization of MTCs in gamma frequency is missing.

https://doi.org/10.7554/eLife.100141.2.sa2

Reviewer #2 (Public review):

Summary

This study provides a detailed analysis and dissociation between two effects of activation of lateral inhibitory circuits in the olfactory bulb on ongoing single mitral/tufted cell (MTC) spiking activity, namely enhanced synchronization in the gamma frequency range or lateral inhibition of firing rate.

The authors use a clever combination of single cell recordings, optogenetics with variable spatial stimulation of MTCs and sensory stimulation in vivo, and established mathematical methods, to describe changes in autocorrelation/synchronization of a single MTC's spiking activity upon activation of other, lateral glomerular MTC ensembles. This assay is rounded off by a gain of function experiment in which the authors enhance granule cell (GC) excitation to establish a causal relation between GC activation and enhanced synchronization of a single MTC's spiking to the gamma rhythm. They had used the same optogenetic manipulation in their previous paper Dalal & Haddad 2022, but use a smaller illumination spot here for spatially restricted activation.

Strengths

This study is of high interest for olfactory processing since it shows directly that interactions between only two selected active receptor channels are sufficient to enhance synchronization of single neurons to gamma in one receptor channel and thus by inference most likely in both. Such synchronization across co-active receptor channels in turn would enable upstream neurons in olfactory cortices to read out odour identity.

The authors find that these interactions are distance-independent over many 100s of µms and thus can allow for non-topographical inhibitory action across the bulb, in contrast to the center-surround lateral inhibition known from other sensory modalities. In my view, analogies between vision and olfaction might have been overemphasized so far, since the combinatorial encoding of olfactory stimuli across the glomerular map might require different mechanisms of lateral interaction versus vision. This result is indicative of such a major difference.

Such enhanced local synchronization to gamma in one channel was observed in a subset of activated channel pairs; in addition, the authors report another type of lateral interaction that does involve reduction of firing rates, drops off with distance and most likely is caused by a different circuit mediated by PV+ neurons (PVN). The evidence for the latter is more circumstantial since no manipulations of PVNs were performed.

Weaknesses/Room for improvement

This study is an impressive proof of concept that however does not yet allow for broad generalization. Thus the framing of results should be slightly more careful IMHO. While the claims in the initial version of this preprint have been toned down quite substantially, the authors do not provide direct hard evidence for synchronization across channels. Admittedly, this would be hard to achieve since it would require paired recordings from MTCs in different locations in vivo. Therefore, the term „lateral synchronization" as it is used in the abstract is still problematic, as well as the title which should rather say „can enable" instead

of „enables". That being said, this study definitely provides important evidence regarding the concept of "lateral synchronization".

The other comments and recommendations have been well taken care of in the new version.

https://doi.org/10.7554/eLife.100141.2.sa1

Author response:

The following is the authors' response to the original reviews.

> ***eLife Assessment***
>
> *This valuable study provides in vivo evidence for the synchronization of projection neurons in the olfactory bulb at gamma frequency in an activity-dependent manner. This study uses optogenetics in combination with single-cell recordings to selectively activate sensory input channels within the olfactory bulb. The data are thoughtfully analyzed and presented; the evidence is solid, although some of the conclusions are only partially supported.*

We deeply thank all the reviewers for their time, effort, and insightful comments. Their revision led to a significant improvement of the paper.

The reviewers suggested toning down our claim that we found a mechanism that synchronizes all odor-evoked MTC activities, as we do not directly show that. We concur and address this in our revised version to ensure a precise interpretation of our findings. In short, we state that we revealed a synchronization mechanism between two groups of active mitral and tufted cells (MTCs) and show that this synchronization is activity-dependent and distance-independent. This mechanism can enable the synchronization of all odor-activated MTCs.

Another issue raised is the interpretation of the results obtained under Ketamine anesthesia. Ketamine is an NMDA receptor antagonist that plays a crucial role in the MTC-GC reciprocal synapse. To address this, we include new analyses demonstrating that optogenetic activation of granule cells (GCs) can inhibit the recorded MTCs during baseline activity but does not substantially affect odor-evoked MTC firing rates. We show that this is correct in both Ketamine-induced anesthesia and awake mice (Dalal & Haddad, 2022). This indicates that GC-MTC connections are functional even under Ketamine anesthesia, however, they do not exert substantial suppression on odor-evoked MTC responses. We added a paragraph to the discussion section on the potential influence of Ketamine anesthesia on GC-MTC synapses and its implications on our findings.

Finally, we discuss several recent studies that are particularly relevant to our research and expand the discussion on our hypothesis that parvalbumin-positive cells in the olfactory bulb may serve as key mediators of the activity- and distance-dependent lateral inhibition observed in our findings.

> ***Public Reviews:***
>
> ***Reviewer #1 (Public Review):***
>
> *Summary:*
>
> *Dalal and Haddad investigated how neurons in the olfactory bulb are synchronized in oscillatory rhythms at gamma frequency. Temporal coordination of action potentials fired by projection neurons can facilitate information transmission to downstream areas.*

> *In a previous paper (Dalal and Haddad 2022, https://doi.org/10.1016/j.celrep.2022.110693), the authors showed that gamma frequency synchronization of mitral/tufted cells (MTCs) in the olfactory bulb enhances the response in the piriform cortex. The present study builds on these findings and takes a closer look at how gamma synchronization is restricted to a specific subset of MTCs in the olfactory bulb. They combined odor and optogenetic stimulations in anesthetized mice with extracellular recordings.*
> *The main findings are that lateral synchronization of MTCs at gamma frequency is mediated by granule cells (GCs), independent of the spatial distance, and strongest for MTCs with firing rates close to 40 Hz. The authors conclude that this reveals a simple mechanism by which spatially distributed neurons can form a synchronized ensemble. In contrast to lateral synchronization, they found no evidence for the involvement of GCs in lateral inhibition of nearby MTCs.*
>
> *Strengths:*
>
> *Investigating the mechanisms of rhythmic synchronization in vivo is difficult because of experimental limitations for the readout and manipulation of neuronal populations at fast timescales. Using spatially patterned light stimulation of opsin-expressing neurons in combination with extracellular recordings is a nice approach. The paper provides evidence for an activity-dependent synchronization of MTCs in gamma frequency that is mediated by GCs.*
>
> *Weaknesses:*
>
> *An important weakness of the study is the lack of direct evidence for the main conclusion - the synchronization of MTCs in gamma frequency. The data shows that paired optogenetic stimulation of MTCs in different parts of the olfactory bulb increases the rhythmicity of individual MTCs (Figure 1) and that combined odor stimulation and GC stimulation increases rhythmicity and gamma phase locking of individual MTCs (Figure 4). However, a direct comparison of the firing of different MTCs is missing. This could be addressed with extracellular recordings at two different locations in the olfactory bulb. The minimum requirement to support this conclusion would be to show that the MTCs lock to the same phase of the gamma cycle. Also, showing the evoked gamma oscillations would help to interpret the data.*

We agree with the reviewer that direct evidence of mutual synchronization between multiple recorded MTCs has not been shown in our study. Our study only shows a mechanism that can enable this synchronization. We now state this clearly in the manuscript. We based this on previous studies that tested MTC spike synchronization. Specifically, Schoppa 2006, reported that electrical OSN stimulation evokes MTC spikes synchronization in the gamma range, in-vitro. Kashiwadni et al., 1999 and Doucette et al., 2011 showed that odor-evoked MTC spike times are synchronized, in-vivo. Given these studies, we asked what is the underlying mechanism that can support such a synchronization. Our study demonstrates that activating a group of MTCs can entrain another MTC in an activity-dependent and distance-independent manner. We claim this could be the underlying mechanism for the odor-evoked synchronization as demonstrated by these previous studies.

To make sure this is clearly stated in the manuscript we changed the title to “Activity-dependent lateral inhibition enables the synchronization of active olfactory bulb projection neurons”, and rephrased a sentence in the abstract to “This lateral synchronization was particularly effective when the recorded MTC fired at the gamma rhythm”. To further clarify this point, we made several other changes throughout the results and the discussion section.

> *Another weakness is that all experiments are performed under anesthesia with ketamine/medetomidine. Ketamine is an antagonist of NMDA receptors and NMDA*

> *receptors are critically involved in the interactions of MTCs and GCs at the reciprocal synapses (see for example Lage-Rupprecht et al. 2020, https://doi.org/10.7554/eLife.63737; Egger and Kuner 2021, https://doi.org/10.1007/s00441-020-03402-7). This should be considered for the interpretation of the presented data.*

This issue has been raised by reviewers #1 and #2. We think, as also reviewer #2 acknowledged, that this issue does not compromise our results. However, to address this important point we added the below section to the Discussion:

"Our experiments were performed under Ketamine anesthesia, an NMDA receptor antagonist that affects the reciprocal dendro-dendritic synapses between MTCs and GCs (Egger and Kuner, 2021; Lage-Rupprecht et al., 2020). Consistent with that, recent studies reported lower excitability of GC activity under anesthesia (Cazakoff et al., 2014; Kato et al., 2012). This raises the concern that our result might not be valid in the awake state. We argue that this is unlikely. First, (Fukunaga et al., 2014) reported that GCs baseline activity in anesthetized and awake mice is similar, suggesting that MTC-GC synapses are functioning. Second, we show that light activation of GCL neurons strongly inhibits the MTC baseline activity (Figure 5) and increases MTC odor-evoked spike-LFP coupling in the gamma range (Figure 4). These experiments validate that GCL neurons can exert inhibition over MTCs in our experimental setup. Third, we have shown that light-activating all accessible GCL neurons has a minor effect on the MTC odor-evoked firing rates in an awake state (Dalal and Haddad, 2022), corroborating the finding that GCL neurons are unlikely to provide strong suppression to MTCs. Fourth, and most importantly, we showed that optogenetic stimulation of MTCs entrains other MTC spike times, which is achieved via the GCL neurons. This suggests that the lack of lateral suppression following MTC or GCL neuron opto-activation is not due to MTC-GC synapse blockage. That said, we cannot exclude the unlikely possibility that NMDA receptor blockage under anesthesia impairs MTC-to-MTC suppressive interactions but not the MTC-to-MTC mediated spike entrainment."

Figure 1A and D from Dalal & Haddad 2022 show the effect of GCL neurons opto-activation during odor stimulation on MTC firing rates in awake and anesthetized mice.

> *Furthermore, the direct effect of optogenetic stimulation on GCs activity is not shown. This is particularly important because they use Gad2-cre mice with virus injection in the olfactory bulb and expression might not be restricted to granule cells and might not target all subtypes of granule cells (Wachowiak et al., 2013, https://doi.org/10.1523/JNEUROSCI.4824-12.2013). This should be considered for the interpretation of the data, particularly for the absence of an effect of GC stimulation on lateral inhibition.*

In this study we used Gad2-cre mice, and the protocol for viral transfection of GCL neurons reported in Fukunaga et al., 2014. They reported that: 'more than 90% of Cre-expressing neurons in the GCL also expressed fluorescently tagged ArchT'. Consistently, when Fukunaga et al. expressed ChR2 in the GCL using the same viral infection as we used, they reported that: "Light presentation in vivo resulted in rapid and strong depolarization of, and action potential (AP) discharges in, GCs (Fig. 3b), which in

turn consistently and strongly hyperpolarized M/TCs (9 of 9 cells showed 100% AP suppression; Fig. 3c,d)". This study shows clearly that this infection protocol is robust. Moreover, in new panels we added to the manuscript (Figure 5a-b), we show that optogenetic activation of GCL neurons strongly suppressed MTC activity during baseline conditions but not odor-evoked responses MTCs. This is consistent with the reports by Fukunaga et al, and indicates that GCL neurons are functional as they can suppress MTC baseline activity.

Finally, since virus injection to the granule cell layer can target other GCL neuron types, we changed the reference in the text to GCL neurons (as was done in Gschwend et al., 2015)

instead of 'GCs' when referring to GC. We replaced the image in Figure 4A, to show the expression of ChR2 is restricted to GCL neurons. That said, it is still possible that our protocol did not infect all GC subtypes. To address this, we added this line to the Discussion: "We also note that our viral transfection protocol in Gad2-Cre mice might not transfect all subtypes of GCs"

> *Several conclusions are only supported by data from example neurons. The paper would benefit from a more detailed description of the analysis and the display of some additional analysis at the population level:*
>
> *- What were the criteria based on which the spots for light-activation were chosen from the receptive field map?*

In order to make this point clearer, we extended the explanation in the Methods on the selection criteria: "Spots were selected either randomly or manually. In the manual selection case, we selected spots that caused either significant or mild but insignificant inhibitory effect on the recorded MTC (e.g., local cold spots in the receptive-field map; see example in Figure 2a of example spots that were selected manually)". We also add a reference in the text to the Methods: "see Methods for spots selection criteria".

> *- The absence of an effect on firing rate for paired stimulations is only shown for one example (Figure 1c). A quantification of the population level would be interesting.*
>
> *- Only one example neuron is shown to support the conclusion that "two different neural circuits mediate suppression and entrainment" in Figure 3. A population analysis would provide more evidence.*

Thank you very much for these comments. We added a population analysis in Figure 3. This analysis shows a dissociation between firing rate suppression and the entrainment groups (Figure 3c-d). This suggests that two different circuits mediate suppression and entrainment.

> *- Only one example neuron is shown to illustrate the effect of GC stimulation on gamma rhythmicity of MTCs in Figures 4 f,g.*

In this figure, we show that the activation of subsets of GCL neurons elevated odor-evoked spike synchronization to the gamma rhythm. We thought it would be beneficial to demonstrate the change in spike entrainment following GCL neurons optogenetic activation regardless of the ongoing OB gamma oscillations, using the method presented by Fukunaga et al., 2014. However, this analysis requires that the neuron has a relatively high firing rate. As we describe in the figure legend of this panel, this neuron is probably a tufted cell based on the findings shown in Fukunaga et al., 2014 and Burton & Urban, 2021. Most of our recorded cells had a lower firing rate, which coincides with our typical recording depth, targeting mitral cells rather than tufted cells (~400µm deep). Since this analysis is shown only over a single neuron, we moved it to Supplementary Figure 4.

> *- In Figure 5 and the corresponding text, "proximal" and "distal" GC activation are not clearly defined.*

We agree. Initially, we used these terms to refer to GC columns that include the recorded MTC (proximal) and columns that are away from it (distal). We decided that instead of using a coarse division, we would show the whole range of distances. We updated the analysis in Figure 5d to show the effect of GC optogenetic activation on MTC odor-evoked responses as a function of the distance from the recorded MTC.

Reviewer #2 (Public Review):

Summary

This study provides a detailed analysis and dissociation between two effects of activation of lateral inhibitory circuits in the olfactory bulb on ongoing single mitral/tufted cell (MTC) spiking activity, namely enhanced synchronization in the gamma frequency range or lateral inhibition of firing rate.

The authors use a clever combination of single-cell recordings, optogenetics with variable spatial stimulation of MTCs and sensory stimulation in vivo, and established mathematical methods to describe changes in autocorrelation/synchronization of a single MTC's spiking activity upon activation of lateral glomerular MTC ensembles. This assay is rounded off by a gain-of-function experiment in which the authors enhance granule cell (GC) excitation to establish a causal relation between GC activation and enhanced synchronization to gamma (they had used this manipulation in their previous paper Dalal & Haddad 2022, but use a smaller illumination spot here for spatially restricted activation).

Strengths

This study is of high interest for olfactory processing - since it shows directly that interactions between only two selected active receptor channels are sufficient to enhance the synchronization of single neurons to gamma in one channel (and thus by inference most likely in both). These interactions are distance-independent over many 100s of µms and thus can allow for non-topographical inhibitory action across the bulb, in contrast to the center-surround lateral inhibition known from other sensory modalities.

In my view, parallels between vision and olfaction might have been overemphasized so far, since the combinatorial encoding of olfactory stimuli across the glomerular map might require different mechanisms of lateral interaction versus vision. This result is indicative of such a major difference.

Such enhanced local synchronization was observed in a subset of activated channel pairs; in addition, the authors report another type of lateral interaction that does involve the reduction of firing rates, drops off with distance and most likely is caused by a different circuit-mediated by PV+ neurons (PVN; the evidence for which is circumstantial).

Weaknesses/Room for improvement

Thus this study is an impressive proof of concept that however does not yet allow for broad generalization. Therefore the framing of results should be slightly more careful in my opinion.

We agree with the reviewer. We copy here our response to reviewer #1, who raised the same issue.

We agree that direct evidence of mutual synchronization between multiple recorded MTCs has not been shown in our study. Our study only shows a mechanism that can enable this synchronization. We now state this clearly in the manuscript. We relayed previous studies that tested MTC spike synchronization. Specifically, Schoppa 2006, reported that electrical OSN stimulation evokes MTC spikes synchronization in the gamma range, in-vitro. Kashiwadni et al., 1999 and Doucette et al., showed that odor-evoked MTC spike times are synchronized, in-vivo. Given these studies, we asked what is the underlying mechanism that can support such a synchronization. Our study demonstrates that activating a group of MTCs can entrain another MTC in an activity-dependent and distance-independent manner. We

claim this could be the underlying mechanism for the odor-evoked synchronization as demonstrated by these previous studies.

To make sure this is clearly stated in the manuscript we changed the title to “Activity-dependent lateral inhibition enables the synchronization of active olfactory bulb projection neurons”, and rephrased a sentence in the abstract to “This lateral synchronization was particularly effective when the recorded MTC fired at the gamma rhythm”. To further clarify this point, we made several other changes throughout the results and the discussion section.

> *Along this line, the conclusions regarding two different circuits underlying lateral inhibition vs enhanced synchronization are not quite justified by the data, e.g.*
>
> *(1) The authors mention that their granule cell stimulation results in a local cold spot (l. 527 ff) - how can they then said to be not involved in the inhibition of firing rate (bullet point in Highlights)? Please elaborate further. In l.406 they also state that GCs can inhibit MTCs under certain conditions. The argument, that this stimulation is not physiological, makes sense, but still does not rule out anything. You might want to cite Aghvami et al 2022 on the very small amplitude of GC-mediated IPSPs, also McIntyre and Cleland 2015.*

We apologize for the lack of clarity. We reported that we found a local cold spot in the context of an additional experiment not presented in the manuscript and only described in the Methods section. Following the revision, we decided to add the analysis of this experiment to Figure 5. This experiment validated that optogenetic activation of GCs is potent and can affect the recorded MTC firing rates. This is particularly important as we performed all experiments under Ketamine anesthesia, which is a NMDA receptor antagonist. In this experiment, we recorded the activity of MTCs at baseline conditions (without odor presentation) under optogenetic activation of GCs. We divided the OB surface into a grid and optogenetically activated GC columns at a random order, one light spot in each trial, using light patches of size of size 330um2. We used the same light intensity as in the optogenetic GC activation during odor stimulation (reported in Figures 4-5). We show that the recorded MTC was strongly inhibited by GC light activation, mostly when activating GCs in its vicinity (within its column, i.e., local cold spot). This experiment validates that in our experimental setup, GCs can exert inhibition over MTCs at baseline conditions.

> *(2) Even from the shown data, it appears that laterally increased synchronization might co-occur with lateral suppression (See also comment on Figures 1d,e and Figure S1c)*

We kindly note that the panels you referred to do not quantify the firing rate but the rhythmicity of MTC light-evoked responses. We should have explained these graphs better in the main text and not only in the Methods section. We added a panel to Supplementary Figure 1, which describes our analysis: In each of these examples, we performed a time-frequency Wavelet analysis over the average response of the neurons across trials (computed using a sliding Gaussian with a std of 2ms). The results of the Wavelet analysis allowed us to visually capture the enhanced spike alignment across trials under paired activation as a function of the stimulus duration (as, for example, in Figure 1c, middle panel). The response amplitude to light stimulation did not change in this example (shown in Figure 1c lower panel), and the spikes entrainment increased following paired activation of MTCs.

To address the relations between lateral suppression and synchronization at the population level, we added additional analyses to Figure 3c-d.

> *(3) There are no manipulations of PVN activity in this study, thus there is no direct evidence for the substrate of the second circuit.*

We completely agree with the reviewer. Using the current data, we can only claim that optogenetic activation of GCL neurons did not affect the MTC odor-evoked response. This finding is consistent with the loss-of-function experiment reported by Fukunaga et al., 2014, where GC suppression did not change odor-evoke responses in both anesthetized and awake mice. Therefore, we speculated that PVN might be a candidate OB interneuron to mediate lateral inhibition between MTCs. This hypothesis is based on their higher likelihood of interconnecting two MTCs compared with GCs (Burton, 2017). We elaborated on this in the discussion and made sure it is clearly stated as a hypothesis.

> *(4) The manipulation of GC activity was performed in a transgenic line with viral transfection, which might result in a lower permeation of the population compared to the line used for optogenetic stimulation of MTCs.*

We used a previously validated protocol for optogenetic manipulation of GCs from Fukunaga et al., 2014 in order to minimize this caveat. As we cited previously from their paper, following the expression of ChR2 in the GCL, 'Light presentation in vivo resulted in rapid and strong depolarization of, and action potential (AP) discharges in, GCs (Fig. 3b), which in turn consistently and strongly hyperpolarized M/TCs (9 of 9 cells showed 100% AP suppression; Fig. 3c,d)'. These results are consistent with the additional experiment we added to the manuscript, where optogenetic activation of GCL neurons strongly suppressed MTC activity during baseline conditions (without odor presentation). The high similarity between these two reports, in which, in the case of Fukunaga et al., GC activation was directly measured, suggests that lack of opsin expression or insufficient light intensity is unlikely to explain the lack of GCL neuron activation effect on lateral inhibition. Moreover, GCL neurons' optogenetic activation during odor stimulation increased MTC spike-LFP coupling in the gamma range. Therefore, the dissociation between the effects of GCL neurons on spike entrainment and lateral inhibition suggests that the lack of lateral inhibition following GC activation is unlikely due to low expression rates.

> *In some instances, the authors tend to cite older literature - which was not yet aware of the prominent contribution of EPL neurons including PVN to recurrent and lateral inhibition of MT cells - as if roles that then were ascribed to granule cells for lack of better knowledge can still be unequivocally linked to granule cells now. For example, they should discuss Arevian et al (2006), Galan et al 2006, Giridhar et al., Yokoi et al. 1995, etc in the light of PVN action.*
>
> *Therefore it is also not quite justified to state that their result regarding the role of GCs specifically for synchronization, not suppression, is "in contrast to the field" (e.g. l.70 f.,, l.365, l. 400 ff).*

We changed several sentences in the discussion and introduction to explain that previous studies attributed lateral suppression to GC because they were not aware of the prominent contribution of EPL neurons as has been demonstrated by more recent studies (Burton 2024, Huang et al., 2016, Kato et al., 2013, and more).

We also toned down the statement that these findings are in contrast to the field. Instead, we state that our findings support the claim that GCs are not involved in affecting MTC odor-evoked firing rate.

> *Why did the authors choose to use the term "lateral suppression", often interchangeably with lateral inhibition? If this term is intended to specifically reflect reductions of firing rates, it might be useful to clearly define it at first use (and cite earlier literature on it) and then use it consistently throughout.*

We agree and have changed the manuscript accordingly. We added the following in the introduction: “We use this phrase here to refer to a process that suppresses the firing rate of the post-synaptic neuron.”

> *A discussion of anesthesia effects is missing - e.g. GC activity is known to be reportedly stronger in awake mice (Kato et al). This is not a contentious point at all since the authors themselves show that additional excitation of GCs enhances synchrony, but it should be mentioned.*

We completely agree and added a paragraph to the Discussion in this regard. Please see also the response to reviewer #1, who made a similar suggestion.

> *Some citations should be added, in particular relevant recent preprints - e.g. Peace et al. BioRxiv 2024, Burton et al. BioRxiv 2024 and the direct evidence for a glutamate-dependent release of GABA from GCs (Lage-Rupprecht et al. 2020).*

We thank the reviewer for noting us these relevant recent manuscripts. We have now cited Peace et al., when discussing the spatial range of inhibition and gamma synchronization in the OB, Lage-Rupprecht et al in the context of the involvement of NMDA receptor in MTC-GC reciprocal synapse and Burton et al. when discussing PV neurons potential function.

> *The introduction on the role of gamma oscillations in sensory systems (in particular vision) could be more elaborated.*

In our previous paper (Dalal & Haddad 2022) we had an elaborated introduction on the role of gamma oscillations in sensory processing, since we focused in this study in the effect of gamma synchronization on information transmission between brain regions. In the current study we looked at gamma rhythms as a mechanism that can facilitate ensemble synchronization.

> ***Reviewer #3 (Public Review):***
>
> *Summary:*
>
> *This study by Dalal and Haddad analyzes two facets of cooperative recruitment of M/TCs as discerned through direct, ChR2-mediated spot stimulations:*
>
> *(1) mutual inhibition and*
>
> *(2) entrainment of action potential timing within the gamma frequency range.*
>
> *This investigation is conducted by contrasting the evoked activity elicited by a "central" stimulus spot, which induces an excitatory response alone, with that elicited when paired with stimulations of surrounding areas. Additionally, the effect of Gad2-expressing granule cells is examined.*
>
> *Based on the observed distance dependence and the impact of GC stimulations, the authors infer that mutual inhibition and gamma entrainment are mediated by distinct mechanisms.*
>
> *Strengths:*
>
> *The results presented in this study offer a nice in vivo validation of the significant in vitro findings previously reported by Arevian, Kapoor, and Urban in 2008. Additionally, the distance-dependent analysis provides some mechanistic insights.*

We thank the reviewer for his comments. Indeed, the current study provides in-vivo replication of the results reported in Arevian et al., 2008 in-vitro, and adds further insights by showing that lateral inhibition is distant-dependent. However, this is not the main focus of the current study. Following the findings reported by Dalal & Haddad 2022, the motivation for this study was to test the mechanism that allows co-activated MTCs to entrain their spike timing. By light-activating pairs of MTCs at varying distances, we detected a subset of pairs in which paired light-activation evoked activity-dependent lateral inhibition, as was reported by Arevian et al., 2008. Moreover, we think it is highly important to know that a previous result in an in-vitro study is fully reproducible in-vivo.

> *Weaknesses:*
>
> *The results largely reproduce previously reported findings, including those from the authors' own work, such as Dalal and Haddad (2022), where a key highlight was "Modulating GC activities dissociates MTCs odor-evoked gamma synchrony from firing rates." Some interpretations, particularly the claim regarding the distance independence of the entrainment effect, may be considered over-interpretations.*

We kindly disagree with the reviewer. We think the current study extends rather than reproduces the findings reported in Dalal & Haddad 2022. The 2022 study mainly focused on the effect of OB gamma synchronization on odor representation in the Piriform cortex. We bidirectionally modulated the level of MTC gamma synchronization and found that it had bidirectional effects on odor representation in one of their downstream targets, the anterior piriform cortex. The current study, however, focuses on the question of how spatially distributed odor-activated MTCs can synchronize their spiking activity. Our current main finding is that paired activation of MTCs can enhance the spikes entrainment of the recorded MTC in an activity-dependent and spatially independent manner. We suggest that this mechanism is mediated by GCL neurons.

The reviewer did not explain why he\she thinks that the distance independence of the entrainment effects is an over-interpretation. However, to make our claim more precise we added the following sentence to the corresponding results section:" Furthermore, within the distance range that we were able to measure, the increased phase-locking did not significantly correlate with the distance from the MTC"

> ***Recommendations for the authors:***
>
> ***Reviewer #1 (Recommendations For The Authors):***
>
> *Minor comments:*
>
> *(1) Line 17f: "This lateral synchronization was particularly effective when both MTCs fired at the gamma rhythm, ..."*
>
> *This sentence implies a direct comparison of the simultaneously recorded firing of MTCs but I could not find evidence for this in this manuscript. I would suggest to change this.*

We thank the reviewer. The sentence was changed to "This lateral synchronization was particularly effective when the recorded MTC fired at the gamma rhythm".

> *(2) Line 43f: A brief description of what glomeruli are could help to avoid confusion for readers less familiar with the OB. The phrasing of "activated glomeruli" and "each glomerulus innervates" are somewhat misleading given that they do not contain the cell bodies of the projection neurons.*

We edited this part of the introduction so it briefly describes what glomeruli are: 'Olfactory processing starts with the activity of odorant-activated olfactory sensory neurons. The axons of these sensory neurons terminate in one or two anatomical structures called glomeruli located on the surface of the olfactory bulb (OB). Each glomerulus is innervated by several mitral and tufted cells (MTCs), which then project the odor information to several cortical regions. '

> *(3) Line 78ff: The text sounds as if glomeruli are activated by the light stimulation but ChR2 is expressed in MTCs, the postsynaptic component of the glomeruli. It would be clearer to refer to the stimulation as light activation of MTCs.*

We corrected this sentence to: 'We first mapped each recorded cell's receptive field, i.e., the set of MTCs on the dorsal OB that affect its firing rates when they are light-stimulated.'

> *(4) Line 90: It would be great to mention somewhere in this paragraph that you are analyzing single-unit data sorted from extracellular recordings with tungsten electrodes.*

We added that to the description of the experimental setup: 'To investigate how MTCs interact, we expressed the light-gated channel rhodopsin (ChR2) exclusively in MTCs by crossing the Tbet-Cre and Ai32 mouse lines (Grobman et al., 2018; Haddad et al., 2013), and extracellularly recorded the spiking activity of MTCs in anesthetized mice during optogenetic stimulation using tungsten electrodes.'

> *(5) Line 97: The term "delta entrainment" could be easily confused with the entrainment of MTCs to respiration in the delta frequency band. Maybe better to use a different term or stick to "change in entrainment" also used in the text.*

We completely agree. The term was changed to "change in entrainment" throughout the manuscript and figures.

> *(6) Line 121f: "Light stimulation did not affect ..." . Should this be "Paired light stimulation did not affect ..."?*

Corrected, thank you.

> *(7) Supplementary Figure 1a: The example is not very convincing. It looks a bit like a rhythmic bursting neuron mildly depending on the stimulation.*

This panel serves to present our light stimulation method. The potency of the light stimulation protocol can be seen in the receptive field maps.

> *(8) Supplementary Figure 1c: Why is there no confidence interval for 'Paired'?*

This panel shows the power spectrum density of the average neuron response across trials computed over the entire stimulus window (100ms). We decided to remove this panel, as panel Figure 1d shows the evolution of the entrainment in time and, therefore, provides better insight into the effect.

> *(9) Line 166f: "... across any light intensities". Maybe better "... for the four light intensities tested"?*

We agree, we changed the text in accordance.

> *(10) Figure 2f: It would be more intuitive to have the x-axis in the same orientation as in 2e.*

Corrected, thank you.

> *(11) Figure 4a: The image in this panel is identical to Figure 1a in Dalal and Haddad 2022 in Cell reports just with a different intensity. The reuse of items and data from previous publications should be indicated somewhere but I could not find it.*

We apologize for this replication. We replaced it with a photo showing a larger portion of the OB, demonstrating the restricted viral expression within the GCL.

> *(12) Line 408ff: A brief explanation for the hypothesis of EPL parvalbumin interneurons as the ones mediating lateral inhibition would be great.*

We agree. We added the following paragraph to the discussion section: “We speculate that MTC-to-MTC suppression is mediated by EPL neurons, most likely the Parvalbumin neuron (PV). This hypothesis is based on their activity and connectivity properties with MTCs(Burton, 2017; Kato et al., 2013; Miyamichi et al., 2013; Burton, 2024). More studies are required to reveal how PV neurons affect MTC activity.”

> *(13) Line 425ff: You show that only activity of high firing rate neurons is suppressed by lateral inhibition, whereas "low and noise MTC responses" are not affected. Wouldn't this rather support the conclusion that lateral inhibition prevents excess activity from the OB?*

We found lateral inhibition was mainly effective when the postsynaptic neurons fired at ~30-80Hz in response to light stimulation. That is, it affects MTC firing in this “intermediate” rate, and to a lesser extent when the MTC have low and very high firing rates. To prevent excess activity, one would expect a mechanism that affects more high firing rates than medium ones. This was demonstrated in Kato 2013 for PV-MTC inhibition

> *(14) Line 387: "..., only ~20% of the tested MTC pairs exhibited significant lateral inhibition." This is higher than the 16% of neurons you reported to have lateral entrainment (line 100). Why do you consider the lateral inhibition as 'sparse' but the lateral entrainment as relevant?*

We apologize for this unclear statement. The papers we cited in this regard (Fantana et al., 2008; Lehmann et al., 2016; Pressler and Strowbridge, 2017) have tested lateral inhibition when the recorded MTC was not active, which resulted in a sparse MTC-MTC inhibition. We validated and replicated these findings in our setup, by systematically projecting light spots over the dorsal OB without simultaneous activation of the recorded MTC and found similar rates of largely scarce inhibition (data not shown). In this study, using spike-triggered average light stimulation protocol and paired activation of MTCs, we found higher rates of lateral inhibition, consistent with the reports by Isaacson and Strowbridge, 1998, Urban and Sakmann, 2002. We changed this paragraph to the following:

“We found that in only ~20% of the tested MTC pairs exhibited significant lateral suppression. This rate is consistent with previous in-vitro studies that found lateral suppression between 10-20% of heterotypic MTC pairs (Isaacson and Strowbridge, 1998; Urban and Sakmann, 2002), and is higher compared to a case where the recorded MTC is not active (Lehmann et al., 2016).”

> ***Reviewer #2 (Recommendations For The Authors):***
>
> *Figure-by-figure comments:*
>
> *(1) Figures 1d,e: both these examples seem to show that the firing rate is decreased in the paired condition? From maxima at 110 to 58 Hz in d and 100 to 48 Hz in e. Please explain (see also comment on Figure S1c).*

Please see the response in the Public Review section, reviewer #2, bullet (2). We also added a panel to Supplementary Figure 1 to better explain this.

> *(2) Figure 1 f The means and SEMs are hard to see. Why is the SEM bar plotted horizontally? Since this is a major finding of the paper, will there be a table provided that shows the distribution of Δ shifts across animals?*

We apologize for the mistake. The horizontal bar was the marking of the mean. Since the SEM is small, we corrected the graph for better visualization of the SEM.

> *(3) Figure 1g Showing the running average of data where there is almost none or no data points (beyond 50 Hz) seems not ideal. Is the enhanced entrainment around 40Hz significant? Perhaps the moving average should be replaced by binned data with indicated n?*

We prefer to show all data points instead of binning the data so the reader can see it all. We agree that such a wide range on the x-axis is unnecessary. We shorten this graph only to include the firing rate range in which the data points ranged.

> *(4) Figure 1h Impressive result!*

Thank you!

> *(5) Figure S1a: since the authors show the respiratory pattern here and there obviously was no alignment of light stimulation with inspiration, was there any correlation between the respiratory phase and efficiency of light stimulation with respect to lateral interactions?*

This is an interesting idea. In Haddad et al., 2013, figure 7, the authors performed a similar analysis, and showed that optogenetic activation of MTCs had a more pronounced effect on firing rate in the respiration phases where the neuron was less firing. However, we haven't quantified the impact of lateral interactions with respect to the respiration phase. That being said, the data will be publicly available to test this question.

> *(6) Figure S1c: Here the shift towards a lower firing rate seems to be obvious (see comment in Figures 1 d and e). Please also show the plot for Figure 1e.*

This panel shows the power spectrum density of the average neuron's response across trials computed over the entire stimulus window (100ms). We decided to remove this panel, as panel Figure 1d shows the evolution of the entrainment in time and, therefore, provides better insight into the effect.

> *(7) Figure 2b: show the same plot also for pair 2? Why is it stated that there is no lateral suppression for lateral stimulation alone, if the MTC did not spike spontaneously in the first place and thus inhibition cannot be demonstrated?*

We use Figure 2b to demonstrate the effect of lateral inhibition, and in Figure 2c we detail the responses under each light intensity for both pairs. We think that showing the mean and SEM for one example is enough to give a sense of the effect, as in Figure 2c we show the average response across time together with significant assessment for each pair (panels without a p-value have no significant difference between the conditions).

However, we agree with the comment on this specific example and therefore deleted this sentence. However, at the population level we found no inhibition when activating the lateral spots, regardless of their firing rates (shown in Supplementary Figure 2a).

> *(8) Figure 2d: why is there no distance-dependent color coding for the significant data points? Or, alternatively, since the distance plot is shown in 2e, perhaps drop this information altogether? Again, the moving average is problematic.*

Distance-dependent color coding is applied to all data points in this panel. Significant data points are shown in full circles and have distance-dependent color coding, which is mainly restricted to the lower part of the distance scale (cold colors).

We used a moving average to relate to the similar result reported in Arevian 2008.In Figure 2e, the actual distance for each data point is indicated on the x-axis.

> *(9) Figure 2f: the diagonal averaging method seems to neglect a lot of the data in Figure S2b, why not use radial coordinates for averaging?*

Thank you for the great suggestion. We indeed performed radial coordinates for the averaging, and the results are more robust and better summarize the entire data.

> *(10) Figure 3: These are interesting observations, but are there cumulative data on such types of pairs? Please describe and show, otherwise this can only be a supplemental observation. Regarding 3b was it always the lower light intensity that resulted in suppression and the higher in sync? Since Burton et al. 2024 have just shown that PVNs require very little input to fire!*

This figure shows several examples of entrainment and inhibition properties. As suggested, we added population analysis (Figure 3c-d). This analysis compares the firing rate changes in pairs that evoked significant suppression or entrainment. First, we found only a few pairs in which paired activation evoked both spikes entrainment and suppression. Second, the mean of firing rate changes of pairs that evoked significant entrainment (N=50, shown in Figure 1f in full circles) is significantly different from the mean of the pairs that evoked significant lateral inhibition (N=51, shown in Figure 2d in full circles).

> *(11) Figure 4: This Figure and the corresponding section should be entitled "Additional GC activation... ", otherwise it might be confusing for the reader. A loss of function manipulation (local GC silencing) would be also great to have! You did this in the previous paper, why not here? Raw LFP data are not shown. In Figure 4e the reported odor response firing rate ranges only up to 40Hz, but the example in g shows a much higher frequency. Is the maximum in 4e significant? (same issue as for Figure 1g).*

We changed the phrase to ‘optogenetic GCL neurons activation’. Unfortunately, we haven’t performed experiments where we suppress GC columns. In the previous paper, we suppressed the activity of all accessible GCs, which resulted in reduced spike synchronization to the OB gamma oscillations. Silencing only the GC column is, we think, unlikely to have a substantial effect, especially if the GCs have low activity (but this needs to be tested).

Furthermore, we added examples of raw LFP data for odor stimulation and odor combined with GCL column activation (see Supplementary Figure 4a).

The instantaneous firing rate is high (~80Hz), however the firing rate values we report in Figure 4e is the average within a window of 2 seconds (the odor duration is 1.5 seconds and we extend the window to account for responses with late return to baseline). The average firing rate of this example neuron in this window was 28Hz.

> *(12) Fig 5: what does "proximal" mean - does this mean stimulation of the GCs below the recorded MTC, that might actually belong to the same glomerular unit?*

Yes, by “proximal” we mean the activation of the GC in the column of the recorded MTC. However, we decided that instead of coarsely dividing the data into proximal and distal optogenetic activation of GCL neurons, we will show the data continuously to show that GC had no significant effect on MTC odor-evoked firing rates regardless of their location (Figure 5d).

A comment on the title:

Please tone it down: "Ensemble synchronization" is a hypothesis at this point, not directly shown in the paper. Also, the paper does not show lateral interactions between odor-activated neurons.

We agree and have rephrased it to “Activity-dependent lateral inhibition enables the synchronization of active olfactory bulb projection neurons ”

> *(1) Figure 1a, 2a scale bar missing.*

Corrected, thank you.

> *(2) Figure 1 c is the "rebound" in the lateral stim trace (green) real or not significant?*

The activity during this rebound is not significantly different than the baseline activity before light stimulation.

> *(3) Figure 2b legend: "lateral alone" instead of lateral?*

We appreciate the suggestion. For simplicity, we will keep it as “lateral”.

> *(4) Figure 2c: some of the data plots seem to be breaking off, e.g. the blue line in the bottom third one.*

This line breaking is due to the lack of spikes in this period. The PSTHs used in all analyses result from the convolution of the spike train with a Gaussian window with a standard deviation of 50ms.

> *(5) Figure 2f: Why is the x axis flopped vs 2d,e?*

This panel was mistakenly plotted that way, and was corrected.

> *Comments on the text:*
>
> *Abstract - we had indicated suggestions by strike-throughs and color which are lost in the online submission system, please compare with your original text:*

> *Information in the brain is represented by the activity of neuronal ensembles. These ensembles are adaptive and dynamic, formed and truncated based on the animals̀ experience. One mechanism by which spatially distributed neurons form an ensemble is via synchronization of their spiking activity in response to a sensory event. In the olfactory bulb, odor stimulation evokes rhythmic gamma activity in spatially distributed mitral and tufted cells (MTCs). This rhythmic activity is thought to enhance the relay of odor information to the downstream olfactory targets. However, how only specifically the odor-activated MTCs are synchronized is unknown. Here, we demonstrate that light optogenetic activation of activating one set of MTCs can gamma-entrain the spiking activity of another set. This lateral synchronization was particularly effective when both MTCs fired at the gamma rhythm, facilitating the synchronization of only the odor-activated MTCs. Furthermore, we show that lateral synchronization did not depend on the distance between the MTCs and is mediated by granule cells. In contrast, lateral inhibition between MTCs that reduced their firing rates was spatially restricted to adjacent MTCs and was not mediated by granule cells. Our findings reveal lead us to propose ? a simple yet robust mechanism by which spatially distributed neurons entrain each other's spiking activity to form an ensemble.*

Thank you. We adopted most of the changes and edited the abstract to reflect the reported results better.

> *"both MTCs fired at the gamma rhythm"/this is at this point unwarranted since the mutual entrainment is not shown - tone down or present as hypothesis?*

We completely agree. This sentence was changed to “This lateral synchronization was particularly effective when the recorded MTC fired at the gamma rhythm, facilitating the synchronization of the active MTC”.

> *l. 28: distance-independent instead of "spatially independent"?*

Corrected

> *l. 46: are there inhibitory neurons in the ONL? Or which 6 layers are you referring to here?*

Corrected to “spanning all OB layers”.

> *l. 49: "is mediated" => "likely to be mediated". Schoppa's work is in vitro and did not account for PVNs, see comment in Public Review.*

Corrected. Indeed Schoppaś work was performed in-vitro. We cite it here since it showed that the synchronized firing of two MTC pairs depends on granule cells.

> *l.52: "method"? rather "mechanism"? "specifically" instread of "only"?*

Corrected.

> *l.52: perhaps more precise: a recent hypothesis is that GCs enable synchronization solely between odor-activated MTCs via an activity-dependent mechanism for GABA-release (Lage Rupprecht et al. 2020 - please cite the experimental paper here). Again. Galan has no direct evidence for GCs vs PVNs, see comment in Public Review.*

Thank you, we updated this sentence here and in the discussion and added the relevant citation.

> *l. 66: spike timings instead of spike's timing?*

Corrected to spike timings

> *l. 67 -71: this part could be dropped.*

We appreciate the suggestion; however, we think that it is convenient to briefly read the main results before the results section.

> *l. 76 mouse instead of mice.*

Corrected.

> *l. 77: for clarification: " a single MTC"?*

In some cases, we recorded more than one cell simultaneously.

> *l. 89: just use "hotspot".*

Corrected

> *l. 97 instead of "change", "positive change" or "increase"?*

We left the word change, since we wanted to report that the change between hotspot alone and paired stimulation was significantly higher than zero.

> *l. 104: the postsyn MTC's firing rate.*

Corrected to MTC instead of MTCs

> *l.108: "distributed on the OB surface" sounds misleading, perhaps "across the glomerular map"?*

Corrected.

> *l. 254: "which the MTCs form with each other"- perhaps "which interconnect MTCs".*

Corrected.

> *l. 270 Additional GC activation.*

Corrected to ‘optogenetic activation of GCL neurons’

> *l. 284 somewhat unclear - please expand.*

Corrected to ‘This measure minimizes the bias of the neuron's firing rate on the spike-LFP synchrony value’.

> *l. 371: no odors in Schoppa et al.*

Corrected to ‘It has been shown that two active MTCs can synchronize their stimulus-evoked and odor-evoked spike timings’

> *l. 406 ff. good point - but where is the transition? How does this observation rule out that GCs can mediate lateral suppression?*

It is an important question. We tested two setups of GCs optogenetic activation, either column activation (in this paper) or the activation of all accessible GCs of the dorsal OB (Dalal & Haddad, 2022). Although the latter manipulation results in significant firing rate suppression, the effect of MTC suppression was relatively small in anesthetized mice and even smaller in awake mice. Optogenetically activating GCs at baseline conditions resulted in a strong suppression of only the adjacent MTCs. Taken together, we think that GCs are capable of strongly inhibit MTCs, but it is not their main function in natural olfactory sensation.

> *l. 422 ff: again, this is a hypothesis, please frame accordingly.*

Corrected to ‘Activity-dependent synchronization can enables the synchronization of odor-activated MTCs that are dispersed across the glomerular map’

> *l. 551 typo.*

Corrected.

> *l 556 ff: Figure 2 does not show odor responses.*

Corrected.

> *l 582: Mix up of above/below and low/high?*

Corrected to ‘The values in the STA map that were above or below these high and low percentile thresholds’

> ***Reviewer #3 (Recommendations For The Authors)**:*
>
> *Line 76: "Ai39" should be corrected to "Ai32".*

Corrected. Thank you.

> *Figure Legends: The legends should describe the results rather than interpret the data. For instance, the legends for Figures 1f, g, and h contain interpretations. The authors should review all legends and revise them accordingly.*

We appreciate the comment. However, we kindly disagree. We don’t see these opening sentences as interpretations but as guidance to the reader. For example, ‘Paired stimulation increases spikes’ temporal precision’ is not an interpretation; instead, it describes the finding presented in this panel. We think that legends that only repeat what can already be deduced from the graph are not helpful and, in many cases, obsolete. Explaining what we think this graph shows is common, and we prefer it as it helps the reader.

> *For Figures 1d and e, it may be beneficial to add the spectrograms for the second stimulation alone.*

We show the stimulation of the hotspot alone and when we stimulate both.
The spectrogram of the lateral alone does not show anything of importance.

> *Figures 1a and 2a: Please add color bars so that readers can understand the meaning of the colors plotted.*

Color bars were added.

> *Figure 3: The purpose of this figure is unclear. Why does the baseline firing rate for the paired activation differ? Is this an isolated observation, or is it observed in other units as well?*

This issue has been raised also by reviewer #2. Attached here is our response to reviewer #2

This figure shows several examples of entrainment and inhibition properties. As suggested, we added population analysis (Figure 3c-d). This analysis compares the firing rate changes in pairs that evoked significant suppression or entrainment. First, we found only a few pairs in which paired activation evoked both spikes entrainment and suppression. Second, the mean of firing rate changes of pairs that evoked significant entrainment (N=50, shown in Figure 1f in full circles) is significantly different from the mean of the pairs that evoked significant lateral inhibition (N=51, shown in Figure 2d in full circles).

> *Figures 4 and 5 data seems to come from the same dataset as in Dalal and Haddad (2022) DOI: https://doi.org/10.1016/j.celrep.2022.110693. For example, the fluorescence image looks identical. If this is the case, the authors may want to state that that the image and and some of the data and analyses are reproduced.*

The recorded data shown in these figures are not reproduced from Dalal & Haddad 2022. We collected this data, using GC-columns activation instead of light activating the entire OB dorsal surface as was done in the 2022 paper.

However, the histology image is the same and we now replaced it with a new image, which shows that the expression is restricted to the GCL.

> *Figure 4d: the authors use the data plotted here to argue that the gamma entrainment is distance-independent. But there is a clear decrease over distance (e.g., delta PPC1 over 0.01 is not seen for distance beyond 1000 m). The claim of distance independence may be an over-interpretation of the data. Peace et al. (2024) also claimed that coupling via gamma oscillations occurs over a large spatial extent.*

From a statistical point of view, we can't state that there is a dependency on distance as the correlation is insignificant (P = 0.86). PPC1 of value 0.01 can be found at 0, 500, and 700 microns. Lower values are found at far distances, but this can result from a smaller number of points. The reduced level of synchrony observed at distances above one mm could be the result of the reduced density of lateral interactions at these distances. That said, we rephrase the sentence to a more careful statement. Please see the rephrased sentence at the Public review section.

https://doi.org/10.7554/eLife.100141.2.sa0